REPORT DOCUMENTATION PAGE

Form Approved
OMB No. 0704-0188

1. AGENCY USE ONLY (Leave blank)	2. REPORT DATE	3. REPORT TYPE AND DATES COVERED
	August 25, 1997	Final Report 4/1/94 - 3/30/97

4. TITLE AND SUBTITLE

Net Shape Forming of Tough Fibrous Monolithic Ceramics

5. FUNDING NUMBERS

N00014-94-1-0278

6. AUTHOR(S)

John W. Halloran

7. PERFORMING ORGANIZATION NAME(S) AND ADDRESS(ES)

University of Michigan
Division of Research Development Administration
1058 Wolverine Tower
3003 South State St.
Ann Arbor, MI 48109-1274

8. PERFORMING ORGANIZATION REPORT NUMBER

9. SPONSORING/MONITORING AGENCY NAME(S) AND ADDRESS(ES)

Steven G. Fishman
Office of Naval Research
800 North Quincy St.
Arlington, VA 22217-5660

10. SPONSORING/MONITORING AGENCY REPORT NUMBER

11. SUPPLEMENTARY NOTES

12a. DISTRIBUTION/AVAILABILITY STATEMENT

Unlimited public availability

12b. DISTRIBUTION CODE

13. ABSTRACT *(Maximum 200 words)*

Significant dimensional changes involving linear expansion and shrinkage of 6% occur during heating of a thermoplastic SiC/ethylene vinyl acetate mixture. Thermal expansion occurs before weight loss begins, and can be quantitatively explained in terms of the thermal expansion behavior of the constituents and the crystallization or melting of the semicrystalline polymer. Irreversible anisotropic displacements occur during the first heating cycle due to relaxation of molding strains. These can be reduced by annealing for periods comparable to the viscoelastic relaxation of the ceramic/polymer system. Shrinkage occurs during the early stages of degradation of EVA. This shrinkage is quantitatively accounted for with volume losses resulting from removal of the EVA. Shrinkage continues as weight loss proceeds and stops only at the point the ceramic particles contact one another. Total displacement behavior is the sum of the shrinkage from weight loss plus the expansion from thermal expansion of the individual components, and can be quantitatively predicted for simple or multi-step heating schedules.

14. SUBJECT TERMS	15. NUMBER OF PAGES
binder, removal, dimension, ceramic composites, fabrication, polymer pyrolysis, binder burnout	101
	16. PRICE CODE

17. SECURITY CLASSIFICATION OF REPORT	18. SECURITY CLASSIFICATION OF THIS PAGE	19. SECURITY CLASSIFICATION OF ABSTRACT	20. LIMITATION OF ABSTRACT
unclassified	unclassified	unclassified	unlimited

GENERAL INSTRUCTIONS FOR COMPLETING SF 298

The Report Documentation Page (RDP) is used in announcing and cataloging reports. It is important that this information be consistent with the rest of the report, particularly the cover and title page. Instructions for filling in each block of the form follow. It is important to ***stay within the lines*** to meet ***optical scanning requirements.***

Block 1. Agency Use Only *(Leave blank)*.

Block 2. Report Date. Full publication date including day, month, and year, if available (e.g. 1 Jan 88). Must cite at least the year.

Block 3. Type of Report and Dates Covered. State whether report is interim, final, etc. If applicable, enter inclusive report dates (e.g. 10 Jun 87 - 30 Jun 88).

Block 4. Title and Subtitle. A title is taken from the part of the report that provides the most meaningful and complete information. When a report is prepared in more than one volume, repeat the primary title, add volume number, and include subtitle for the specific volume. On classified documents enter the title classification in parentheses.

Block 5. Funding Numbers. To include contract and grant numbers; may include program element number(s), project number(s), task number(s), and work unit number(s). Use the following labels:

C	- Contract	**PR**	- Project
G	- Grant	**TA**	- Task
PE	- Program Element	**WU**	- Work Unit Accession No.

Block 6. Author(s). Name(s) of person(s) responsible for writing the report, performing the research, or credited with the content of the report. If editor or compiler, this should follow the name(s).

Block 7. Performing Organization Name(s) and Address(es). Self-explanatory.

Block 8. Performing Organization Report Number. Enter the unique alphanumeric report number(s) assigned by the organization performing the report.

Block 9. Sponsoring/Monitoring Agency Name(s) and Address(es). Self-explanatory.

Block 10. Sponsoring/Monitoring Agency Report Number. *(If known)*

Block 11. Supplementary Notes. Enter information not included elsewhere such as: Prepared in cooperation with...; Trans. of...; To be published in.... When a report is revised, include a statement whether the new report supersedes or supplements the older report.

Block 12a. Distribution/Availability Statement. Denotes public availability or limitations. Cite any availability to the public. Enter additional limitations or special markings in all capitals (e.g. NOFORN, REL, ITAR).

- **DOD** - See DoDD 5230.24, "Distribution Statements on Technical Documents."
- **DOE** - See authorities.
- **NASA** - See Handbook NHB 2200.2.
- **NTIS** - Leave blank.

Block 12b. Distribution Code.

- **DOD** - Leave blank.
- **DOE** - Enter DOE distribution categories from the Standard Distribution for Unclassified Scientific and Technical Reports.
- **NASA** - Leave blank.
- **NTIS** - Leave blank.

Block 13. Abstract. Include a brief *(Maximum 200 words)* factual summary of the most significant information contained in the report.

Block 14. Subject Terms. Keywords or phrases identifying major subjects in the report.

Block 15. Number of Pages. Enter the total number of pages.

Block 16. Price Code. Enter appropriate price code *(NTIS only)*.

Blocks 17. - 19. Security Classifications. Self-explanatory. Enter U.S. Security Classification in accordance with U.S. Security Regulations (i.e., UNCLASSIFIED). If form contains classified information, stamp classification on the top and bottom of the page.

Block 20. Limitation of Abstract. This block must be completed to assign a limitation to the abstract. Enter either UL (unlimited) or SAR (same as report). An entry in this block is necessary if the abstract is to be limited. If blank, the abstract is assumed to be unlimited.

NET SHAPE FORMING OF TOUGH FIBROUS MONOLITHIC CERAMICS an AASERT Project

Contract Number N00014-94-1-0278

Office of Naval Research

ONR Scientific Officer: Steven G. Fishman
01 April 1994- 30 March 1997

Final Technical Report
August 25, 1997

Principal Investigator: John W. Halloran
Department of Materials Science and Engineering
University of Michigan
Ann Arbor, MI 48109-2136

NET SHAPE FORMING OF TOUGH FIBROUS MONOLITHIC CERAMICS
Final Technical Report

Abstract

ONR Contract Information is summarized below
Contract Title: Tough Ceramics from Fibrous Monoliths
Performing Organization: University of Michigan
Principal Investigator: John W. Halloran
Contract Number: N00014-94-1-0278
ONR Scientific Officer: Steven G. Fishman

A. Scientific Research Goals

This is the final technical report for an AASERT program N00014-94-1-0278 "Net Shape Forming of Tough Fibrous Monolithic Ceramics", which is an augmentation of the Grant N00014-91-J-1999 concerning advnced development and scale-up of fibrous monolithic ceramics. The AASERTS student was to establish the feasibility of net shape forming by studying pressureless sintering of fibrous monoliths

The first key problem was to assure that all large voids are fully collapsed during consolidation, and that the part survives binder removal and densification. The AASERTS student will determine the time-temperature-section thickness processing envelope for the existing powder-polymer systems and evaluate new polymer systems, offering improved burnout behavior while still maintaining processibility.

B. Significant Results from the Program

This AASERTS program became the PhD Thesis of Kenneth Hrdina "Phenomena During Thermal Removal of Binders". Hrdina studied in detail the ethylene vinyl acetate copolymer used in fibrous monoliths. He determined that the origin of binder removal problems was the evolution of gaseous acetic acid during the very early stages of the process. This process was examined in detail, as reported in "Chemistry of Removal of Ethylene Vinyl Acetate Binders", (K.E. Hrdina and J. W. Halloran, Massoud Kaviany, and Amir Oliveira, Submitted to J. Materials Science July 1997).

This process was successfully modeled, leading to a predictive model minimizing the time required for safe burnout. The mechanism of defect formation, and the transport model of burnout are reported in "Defect Formation During Binder Removal of Ethylene Vinyl Acetate Filled Systems" (K.E. Hrdina and J. W. Halloran, Massoud Kaviany, and Amir Oliveira, Submitted to J. Materials Science July 1997). Other papers on this topic are in preparation.

Hrdina built a unique thermomechanical analyzer, which allowed him to follow precisely the dimensional changes during binder removal. We believe this is unique. The data showed a surprising set of behaviors, including reversible and irreversible relaxations, significant expansions, and contraction during the removal stage. These are described and quantitatively modeled in "Dimensional Changes During Binder Removal in a Moldable Ceramic System" (K.E. Hrdina and J. W. Halloran Submitted to J. Materials Science July 1997)

These bulk of this report are manuscripts of these papers, which are included as an appendix.

Appendix

This Appendix includes copies of the manuscripts of three of the principal publications resulting from this research grant. These are:

K.E. Hrdina and J. W. Halloran "Dimensional Changes During Binder Removal in a Moldable Ceramic System", Submitted to J. Materials Science (July 1997)

K.E. Hrdina and J. W. Halloran, Massoud Kaviany, and Amir Oliveira "Chemistry of Removal of Ethylene Vinyl Acetate Binders", Submitted to J. Materials Science (July 1997)

K.E. Hrdina and J. W. Halloran, Massoud Kaviany, and Amir Oliveira "Defect Formation During Binder Removal of Ethylene Vinyl Acetate Filled Systems", Submitted to J. Materials Science (July 1997)

Dimensional Changes During Binder Removal in a Moldable Ceramic System

Kenneth E. Hrdina and John W. Halloran
University of Michigan

INTRODUCTION

Certain ceramic fabrication techniques, notably thermoplastic injection molding, employ a substantial fraction of polymer binder. We report here observations of significant dilation and contraction of formed ceramics during heating through the binder removal stage. Although the dimensional tolerances of thermoplasticly molded ceramics are very important, dimensional changes in the early stages of binder removal have not been fully appreciated. Few researchers have focused on the dimensional changes that occur during binder removal and none have quantitatively described the whole displacement behavior. It is inconvenient to observe dimensional changes during binder burnout, since the specimen is soft and the noxious effluents produced during binder removal tend to ruin delicate experimental instruments. A thermomechanical analyzer (TMA) which was specifically designed for the binder removal process was built. This TMA applies a very small load to the sample so that dimensional changes can be measured in soft samples undergoing binder removal.

Anisotropic thermal expansion was observed in molded cylinders by Zhang and Evans [1]. After annealing, the thermal expansion was isotropic, indicating the presence of residual stresses in the unannealed specimens which qualitatively explained the anisotropy. We report similar residual anisotropic strains in this paper. Edirisinghe and Evans [2] noted that the large dimensional changes occurring within crystalline polymers during cooling was associated with void or microcrack formation.

The thermal removal of ethylene co-vinyl acetate has been studied by Trunec and Cihlar [3] for EVA- paraffinic wax binders with submicron alumina. They report that inert atmospheres are best for removing EVA. A vacuum promotes defect formation through boiling of low molecular weight constituents, while oxygen preferentially degrades the surface regions of the specimen and promotes non-uniform shrinkage. Inert atmospheres minimize the non-uniform shrinkage and thus produced defect-free parts. Earlier work by Wright et al. noted that increases in packing density were observed in parts that underwent uniform degradation procedures, such as in inert atmospheres [4]. It is for this reason that inert atmospheres were used in the present research.

Our observations are schematically illustrated in Fig. 1, a hypothetical displacement history during heating of a molded ceramic specimen. Note that these displacements are large compared to a typical tolerance for finished ceramic parts (0.5-3.0%). Such dimensional changes, especially if anisotropic, could limit achievable tolerance. The initial expansion observed in Fig. 1 occurs as a result of the large thermal expansion of the polymer without much binder loss. Anisotropic expansion may occur at this stage due to

residual strains remaining from molding. The rate of binder removal increases at higher temperatures. Shrinkage occurs as the binder begins to degrade and the volume of material leaving the system is occurring at a faster rate than the volume increases from thermal expansion of the material. Once the temperature for densification is achieved, the part shrinks. Some small thermal shrinkage may occur during cooling to room temperature from the sintering temperature.

EXPERIMENTAL PROCEDURES

Composition and processing

The thermoplastic ceramic system examined here is ethylene co-vinyl acetate[1] (a co-polymer commonly called ethylene vinyl acetate or EVA) blended with ceramic powders consisting of 90 weight percent silicon carbide[2], 6 weight percent aluminum oxide[3] and 4 weight percent yttrium oxide[4]. This SiC composition liquid phase sinters at 1880°C [5-6]. Certain samples also were blended with heavy mineral oil[5], a paraffinic distillate. Some of the properties of the EVA polymer are presented in Table I.

The ceramic powders were mixed by ball milling in isopropanol for 24 hours, using alumina grinding media, followed by drying. Blending of the powder with the resin is done in a heated shear mixer[6] with roller blades. The EVA resin is added first and melted under shear at 130°C at a constant speed of 60 RPM. The ceramic powder is added in small increments of mixing for 1-2 minutes. The increased shear, upon adding the powder, increases mixing temperatures to 150-160°C. The mineral oil, if used, is added next.

The polymer-ceramic powder composition is reported as a nominal room temperature volume percent, based on the room temperature densities of the components. The compositions are 51 volume percent ceramic powder + 49 volume percent co-polymer for the ceramic/EVA system, or 54.5 vol.% ceramic + 39.5 vol. % EVA + 6 vol. % mineral oil for the systems containing mineral oil.

The actual weight percent of binder in each material was determined by thermogravimetric analysis[7] (TGA). Binder uniformity in a batched material and between batches of material was checked by the random selection of four specimens from two

---

[1] ELVAX 470, Dupont.
[2] B-SiC, H.C. Starck Grade B 10; SA = 14-17 m^2/g, mps = 0.75 um.
[3] Malakoff Industries, Inc., RC-HP DBM; SA=7-8 m^2/g, mps = 0.55 um.
[4] Johnson Matthey, mps = 1-2 um.
[5] Heavy Mineral Oil, Mallinckrodt, Paraffin Oil, sp. = 0.881.
[6] C.W. Brabender Instruments, Inc., PL 2000 Plasti-Corder with Roller Blade Mixing Heads.
[7] TGA-171, ATI-CAHN microbalance.

separate batches of material.. These results indicate no significant differences between binder content within a batch of material or between batches. Disc-shaped specimens were fabricated by compression molding in a 25.4 mm diameter uniaxial die[8] at 27 MPa and 125°C. TGA analysis on molded specimens showed that the binder distribution was uniform throughout the sample.

Displacement measurements

Dimensional changes were measured in a TMA designed specifically for studying the binder removal process of thermoplastic ceramics. Fig. 2 is a schematic of the instrument. The specimen rests on a platform at the bottom of an inner fused silica tube. A fused silica rod rests on top of a porous fused silica plate which in turn, rests on the specimen. The porous fused silica plate has 90-150 μm pores to allow unimpeded binder removal while distributing the load that the rod places on the soft specimen. This plate reduces the pressure on the specimen during the test to about 1.4 kPa, so that deformation of the soft specimen is negligible. The LVDT core is attached to the push-rod, and the LVDT bore resides on a fused silica support above the furnace. Elaborate cooling means were used to thermally isolate the specimen from the LVDT core system to localize all dimensional changes to that of the specimen alone. A blank run from RT to 500°C produced a displacement of only plus or minus 1 μm.

Nitrogen gas flows through the inner tube down to the specimen and then up through the annulus between the inner and outer tube to the exhaust port. The TMA is capable of operating from room temperature to temperatures over 800°C in controlled atmospheres. The TMA was calibrated against a single crystal sapphire alumina specimen and was found to be accurate to 0.2 ppm from room temperature to 500°C.

Dimensional and weight loss measurements during binder removal were made on 3 mm thick molded specimens. The specimens were sandwiched between a quartz disk on bottom with a porous quartz disk placed on top of the specimens to both distribute the load and allow gas escape. The weight of the LVDT core and rod produced a nominal pressure of 1.4 kPa. Nitrogen was circulated past the specimen during heating. Weight loss measurements were made by the placement of duplicate specimens with duplicate quartz disks above and below the specimen in a TGA[9] heated at the same schedule as the TMA.

Rheological measurements

---

[8] Leco Corporation, Leco Model 800-200.
[9] TGA-171, ATI-CAHN microbalance.

A cone and plate rheometer[10] was used for determine of relaxation times as a function of both temperature and composition for the polymer and filled polymer. Specimens of the compositions listed in Table II were examined at temperatures of 110, 125, 135, 150 and 170°C. These temperature were above the melting point of the polymer (~85-100°C) but below the temperature at which appreciable degradation occurs (~190°C). The tests were run at a constant stress level with strain measured.

RESULTS AND DISCUSSION

Removal of the EVA

As discussed in detail elsewhere [7,8], EVA removal occurs in two distinct steps. As shown in Fig. 3, no weight loss occurs below 250°C. Around 270°C, the vinyl acetate elimination begins, which produces acetic acid. The acetic acid product is initially dissolved in the polymer, but diffuses to the surface where it is lost as gas. The solid residue of the EVA after acetate elimination is poly ethylene-co-polyacetylene. Acetic acid elimination is complete above 370°C. Degradation of the poly ethylene-co-polyacetylene begins around 400°C and is complete at 500°C. The displacement behavior is examined considering first the events which occur at relatively low temperatures before appreciable binder (~1%) has been removed. Later we will discuss events which occur at higher temperature, where significant amounts of binder are being removed.

Fig. 4 shows the displacement observed for a molded specimen of SiC in EVA and mineral oil upon thermal cycling between RT and 220°C, before EVA degradation begins. There is unique displacement behavior taking place upon initial heating. The displacement is large (6 linear percent) and anisotropic, with expansion occurring in the axial direction of the specimen and contraction occurring in the radial direction of the specimen. The anisotropic displacement only occurs during the first heating cycle. Upon subsequent cooling and heating, the specimen undergoes isotropic displacement. It should again be noted that both the reversible and irreversible displacement so far mentioned is occurring before any appreciable weight loss takes place. The reversible and irreversible displacements will be discussed separately.

Reversible displacement (before EVA removal begins)

The TMA data for one reversible thermal cycle is shown in Fig. 5 for a SiC filled sample with EVA and mineral oil. This section is concerned with the explanation of this phenomenon and its effect on binder removal. The expansion is quite large -- about 4% --

---

[10]Bohlin CS-50 Rheometer.

and there is a change in slope occurring at about 90°C in the heating cycle and about 75°C in the cooling cycle. This is the result of the melting and crystallization of the semicrystalline polymer. Differential Scanning Calorimetry (DSC) measurements were carried out to determine if the melting and crystallization temperatures of the EVA polymer correlated with the behavior observed in the TMA. Fig. 6 shows both DSC and TMA data between 40°C and 120°C for another sample of SiC-filled EVA with mineral oil. This DSC behavior is characteristic of polymeric melting and crystallization. The crystallization process is offset to lower temperatures from that of the melting process which is a result of the time dependent nucleation process for crystallization. It is evident that the melting and crystallization temperatures observed in the DSC correlate with the behavior observed in the TMA.

The next task was to determine how well the measured thermal expansion behavior of these filled polymers compared to those calculated assuming an ideal rule of mixtures for thermal expansion of a composite of ceramic powders in this polymer. For this we use literature data for the thermal expansion of each phase and their volume fractions. The fraction of the crystalline portion of the EVA co-polymer was from DSC experiments, using the enthalpy from the cooling cycle as a measure of the volume fraction crystalline EVA. Using a value of 287J/g for the enthalpy of fusion (ΔH_f) of crystalline polyethylene [9], we infer the fraction the EVA which is crystalline from the ratio of $\Delta H_{measured}$ and ΔH_f, a standard method [9]. The DSC results are summarized in Table III for four different types of samples. The third and fourth sample types were required for application of the ideal rule of mixtures while the other two sample types were run in order to study the effect of the addition of mineral oil and ceramic powder on crystallization in the EVA system.

The percent crystallinity in the pure EVA copolymer (Type I) is about 10%. The addition of mineral oil resulted in a -2°C shift in the T_m and T_c temperatures, indicating some miscibility between mineral oil and EVA copolymer (Type II) [10,11]. However, the mineral oil apparently did not affect the quantity of crystals formed in the copolymer blend. Within the fully loaded polymer systems (Types III and IV), the crystallinity is reduced from 10% in the neat copolymer to between 6.2 and 6.8% in the specimens containing the 50 plus volume percent ceramic powder. Fillers are known to effect crystallinity in a polymer [9,12]. The effect is dependent on both the quantity of filler as well as the interaction between the powder's surface and the polymer. Reduced crystallinity is indication of "strong" interactions between the polymer and the ceramic which inhibits crystallization. The reduced melting point from 90°C for neat EVA to 85°C for the filled polymer indicates that the crystal growth rate has also been reduced in the presence of the filler [12].

The effective quantity of each phase is summarized in Table IV for the two filled systems whose thermal expansion behaviors were shown in Fig.'s 5 and 6. EVA is a random copolymer composed of 82 weight percent polyethylene and 18 weight percent polyvinyl acetate. The thermal expansion values for EVA were obtained through application of the ideal rule of mixtures with thermal expansion data used from both polyvinyl acetate (PVA) and polyethylene (PE). The thermal expansion behavior of petroleum distillates such as mineral oil depends on the specific gravity of the liquid [13,14]. The thermal expansion of mineral oil was taken as the expansion value for a petroleum distillate with the same density (API density = 30 [15])[12].

Fig. 7 shows the results comparing the measured thermal expansion behavior to the values calculated using the rule of mixtures for the specimens with mineral oil. An ideal rule of mixtures agrees well with the experimental behavior of the specimen with mineral oil. Similar results were obtained for the specimen without mineral oil. Additional details are reported elsewhere [7]. The ideal rule of mixtures quantitatively describes the reversible displacement behavior. It should be noted that the ideal rule of mixtures assumes that no strains either build up as a result of thermal expansion mismatch between the phases or are present prior to thermal expansion measurements. Residual strains were relieved, in this case, during the first thermal cycle.

Effect of temperature on the volume fraction of ceramic powder

The volume fraction of ceramic powder, ϕ, is usually considered to be a temperature-independent compositional variable, but in fact it has a significant temperature dependence. The reported value of 54.5 volume percent solids loading is for room temperature only. As the batched material is heated, the polymer expands about 25 to 50 times more than does the ceramic phase. This leads to a decrease in the volume percent of solids as the material is heated. Fig. 8 shows how the volume percent solid loading changes during heating of a specimen within the lower temperature region before appreciable binder removal takes place. It is seen that increasing the temperature significantly lowers the filler level. The volume percent solids loading drops by about 6% in this particular case, when heated from room temperature to the molding temperature (125-150°C). The implications of this on rheological processes is discussed elsewhere [7].

Irreversible displacement (before EVA removal begins)

Recall from Fig. 4 that irreversible displacements were observed during the first heating cycle for the compression molded discs, which featured extra axial expansion in the compression direction and contraction in the radial direction. The irreversible displacement

involves viscoelastic relaxation phenomena. We digress at this point to discuss the viscoelastic behavior of the ceramic-filled EVA.

The compliance response of the SiC/EVA, determined by cone and plate stress relaxation at 125°C is shown in Fig. 9. This shows the long term steady state creep at long times as well as the delayed elastic response or viscous response $\Delta J(t)$. Similar data were obtained at 110, 125, 135, 150, and 170°C, and used to determine the relaxation time vs. temperature. A relaxation time, τ_{relax}, was obtained by assuming a simple exponential relationship in which

$$\Delta J(t) = J_o \exp(-t/\tau_{relax})$$

where t is time, $\Delta J(t)$ is the delayed viscous compliance, and J_o is the limiting recoverable compliance. This fit provides a remarkable representation of the data with a single relaxation time. The y-intercept of the plot also provides information about the instantaneous strain response of the system to an applied shear stress.

A fairly large instantaneous strain relief is coupled with the time dependent relaxation process in the current system. The instantaneous strain relief as a function of temperature and composition is plotted in Fig. 10. It is not surprising to see that the instantaneous amount of strain relieved is not appreciably affected by temperature or mineral oil content. This simply indicates that the elastic portion of the material is not significantly affected by either temperature or mineral oil content.

The filler increases the amount of relieved instantaneous strain from 20 -30 % for the unfilled polymer to 50-70% for the filled polymer. This is perhaps the result of increasing the volume fraction of material that behaves in a hookian manner, i.e., the ceramic filler content. Larger instantaneous relieved strains are desirable since this minimizes the amount of possible residual strains remaining from specimen molding.

The relaxation times as a function of temperature and mineral oil content are plotted in Fig. 11. The relaxation time is about 2.5 minutes at 110 °C and 1 minute at the molding temperature of 125°C for the unfilled polymer. The introduction of the ceramic powder increases this relaxation time to about 8 minutes. It is also evident from Fig. 11 that neither temperature nor mineral oil content drastically changed the relaxation time in the system which initially sounds counter-intuitive. Shorter relaxation times might be expected at higher temperatures or with increased mineral oil where increased polymer mobility occurs, but the data shows that this is not the case. This point deserves some comment. The relaxation time, τ, is related to the ratio of the composite viscosity, η_c, to the composite shear modulus, G_c:

$$\tau \propto \eta_c/G_c$$

The literature for filled polymers [16-18] indicates that the shear viscosity and shear modulus of the matrix phase and the filled composite system are related by:

$$\eta_c/\eta_m \approx G_c/G_m$$

where m and c denotes the matrix phase and composite phases respectively. This is true when the matrix phase is softer than that of the filler and when the Poisson's ratio is 0.5. The polymer is obviously softer than the ceramic material in the current system and the Poisson's ratio is typically 0.5 at temperatures above T_m for polymers [16-18] so that the above conditions for application of Equation 6 are likely fulfilled. Therefore, the trend in the relaxation time can be approximated by observing the trend in matrices behavior from:

$$\tau \propto \eta_c/G_c \approx \eta_m/G_m$$

This indicates that the relaxation time depends on the mobility of the polymer and on its stiffness. The shear modulus and viscosity of the neat polymer was measured at various temperatures. The ratios of the polymer viscosity to shear modulus appear in Fig. 12 and show very little temperature dependence on relaxation time. This was indeed observed as was shown in Fig.'s 10 and 11. It is not surprising, in view of these results, that relaxation time is almost independent of temperature. A similar effect is therefore expected with changes in mineral oil content.

Correlating mold anneal time with irreversible displacement

The extent of irreversible expansion varied with molding conditions such as time at pressure and cooling rate. Specimens were fabricated using the four different molding conditions chosen to elucidate the origin and approximate magnitude of the anisotropic residual strains present in the molded material. All samples were heated at 7°C/min. to 125°C, where a pressure of 27 MPa was applied. Specimen 1 was held under pressure for only 1 minute and rapidly cooled at 23°C/min. Specimen 2 held under pressure for 5 minutes, then rapidly cooled. Specimen 3 was held under pressure for 5 minutes, followed by a 10 minute anneal at 125°C (no pressure), then rapidly cooled. Specimen 4 was the same as Specimen 3, but slowly cooled at 1.6°C/min.

Fig.'s 13a through 13d show the TMA results of these four tests. The unique axial expansion behavior is seen during initial heating for each of the four different respective specimens. The magnitude of the irreversible displacement was largest for Specimen 1 with a 2% irreversible linear expansion, compared to a 1% expansion for the other three specimens. There is little difference between the other three specimens (Fig.'s 13b through 13d), so cooling rate or increasing annealing time from 5 to 15 minutes has little effect. It appears that the filled polymer system has some memory of its previous shape that was not erased in the one minute during molding, but an extra 5 to 15 minutes anneal cut

the irreversible expansion in half. This corresponds to the 8 minute relaxation time calculated from the cone and plate rheometer data.

The glass transition temperature (T_g) of the unfilled EVA polymer is -40°C. The irreversible displacement occurs when a molded specimen is reheated to about 90°C, which is above the melting point of the polymer (Table III). This indicates that the crystallization process has inhibited polymer movement. The filler itself may also contribute, in part, to the immobilization process [12,19]. DSC indicates significant interactions between the polymer and the ceramic as seen by the shift in T_m. Additionally, the quantity of filler and surface area of filler is quite large. Based on the surface area of the powder and volume fraction of filler, the average distance between powder particles is only 19.4 nm. This is on the order of the diameter of gyration of the EVA 470 which is calculated to be between 10 to 16 nm. It is likely that the ceramic filler contributes to the immobilization process in the polymer. The polymer crystallites, present as 6% of the polymer phase also exists in the small 19.4 nm spacing between particles. It is not surprising to see immobilized polymers at temperatures below the T_m of the polymer.

Displacement during binder removal

The displacement behavior from room temperature to 500°C is shown in Fig. 14a, as a plot of displacement and temperature vs. time for the complete binder removal process. This sample had a simple heating profile with two ramp rates. After thermally expanding by almost 6% after 20 hours, the specimen begins to shrink. The shrinkage continues for another 20 hours, then stops for the remaining 8 hours of heating. The net dimensional change of the sample is only -0.5%, compared to the original as-molded dimension. However, the shrinkage is -7.0% with respect to the point of maximum expansion.

Fig. 14b displays the same data as displacement versus temperature for the same 2-ramp heating process. Note that most of the shrinkage occurs in two narrow temperature ranges around 300°C and 380°C. Also shown in Fig. 14b is the weight loss data for a similar TGA sample with the same 2-ramp process. Most of the expansion occurs before weight loss begins. The 300°C shrinkage coincides with first stage weight loss and the 380°C shrinkage coincides with second stage weight loss behavior. Note also the small displacement that occurs at 38 hours in Fig. 14a. This was observed in many samples. It may be associated with intrusion of porosity into the sample, which causes similar displacements during drying[20].

The displacement and weight loss data are combined in Fig. 15 showing displacement versus the fraction of organics which have been removed. Each experimental point represents a different temperature, which is shown for a few points. After the initial

thermal expansion, the sample shrinks as polymer is removed. Shrinkage continues until about 30 percent of the organics have been removed. We presume this point is analogous to the critical point in drying[21]. No porosity forms before the critical point. Porosity develops beyond the critical point.

The entire displacement behavior of filled polymers within the initial stage of binder removal is actually the result of two competing phenomena. First, the specimen expands as a result of thermal expansion with increasing temperature and additional expansion as a result of the semicrystalline polymer melting. The second competing phenomena is the shrinkage resulting from evaporation of the evolving species. The total observed displacement is the sum of the expansion and shrinkage. During initial heating to about 250°C, there is little weight loss, so expansion occurs. At higher temperatures, the binder is removed with very little increase in temperature and shrinkage dominates. Shrinkage continues until the ceramic particles directly contact other ceramic particles. At this point, further shrinkage is prevented.

Also shown on Fig. 15 are theoretical calculations of displacement calculated with the assumption that displacement is a sum of the two terms mentioned above. The first term, the thermal expansion, was calculated using the ideal rule of mixtures as described previously. The second term, the volume shrinkage, needed to take into account the volume of material removed at the temperature at which the material was removed. This was calculated from the weight loss and density at temperature. The details are reported elsewhere [7]. The theoretical calculations involved no adjustable parameters, and were based on the following assumptions: (1) The thermal expansion behavior of amorphous PVA and PE could be extrapolated through all temperatures used. (2) No porosity develops. (3) Weight loss behavior in TMA was same as in TGA indicating no temperature difference between specimens. These assumptions appear to be valid since the two curves match quite well as seen in Fig. 15. Therefore, displacement behavior of the entire binder removal process is quantitatively described.

As previously noted, the polymer phase expands much more than that of the ceramic phase during heating. This has lead to a decrease in the volume percent of solids as the material is heated. Fig. 16 shows the change in volume percent solids loading during the entire binder removal process for a specimen with 51% ceramic + 49% EVA and another with 54.5% ceramic+39.5% EVA +6% mineral oil (all compositions as room temperature volume percent). The initial drop in solids loading is a result of the polymer preferentially thermally expanding more than the ceramic phase. The solids loading again increases as polymer removal proceeds and polymer is removed. Note that the ceramic content drops (in the second case) from 54.5% down to 47%, then increases to about 55%,

a traverse of 7.7 volume percent with relatively little net change after the binder is gone. Such dimensional changes would usually go unnoticed. At the minimum of ceramic volume fraction, the green ceramic should be quite soft. While we have no data on the actual mechanical properties of the ceramics during burnout, we can speculate that the temperature range of minimum ceramic volume fraction is where the risk of slumping is severe.

Effect of heating schedule on displacement history

Typically in ceramic practice, the binder removal schedule is a sequence of ramps instead of the simple 2-ramp schedule discussed previously. A typical multi-step series of eight ramps and seven isothermal holds is shown in Fig. 17 with the resultant displacement and weight loss behavior during the entire binder removal process. Fig. 17a displays displacement vs. time, and Fig. 17b shows displacement vs. temperature. The peaks in the displacement vs. time occur due to thermal expansion during ramps. The sharp drops in displacement vs. temperature reflect shrinkage as material is removed during isothermal holds. Isothermal holds result in weight loss with no temperature change. The theoretically predicted and experimentally observed displacement behavior for this heating schedule is shown in Fig. 18. The theory agrees well with the observed displacements for the 195°C isotherm and the 260°C isotherm, but deviates from the observed shrinkage at the 300°C isotherm. It is common practice in ceramics to design binder removal schedules from TGA weight loss data, choosing slow heating at points of rapid weight loss to avoid defects. It is clear from the TMA displacement data that the ceramic bodies are also actively expanding and contracting, and this may be important in common mechanical defects such as warping and cracking.

Fig. 19 illustrates how the heating schedule can change the displacement history and final density after binder removal. It compares a plot of ceramic volume fraction vs. percent organics removed for two heating schedule. Schedule #1 is a simple schedule with heating at 120°C/hour to 260°C, hold 2 hr, heat 6°C/hr to 450°C. Schedule #2 is the multi-step schedule illustrated in Fig. 17. These two schedules create different paths of density vs. organic content. The multistep schedule avoids the minimum in ceramic density in the early stage of removal, but has a slightly lower density after the dimensional changes stop. The density of both specimens after the binder has been removal is essentially the same as the starting density.

Normal binder removal schedules use fast heating rates during cooling from the mold and fast heating rates up to the temperature at which binder removal starts. This minimizes process time. However, the results in this research suggest that minimum time

may be purchased at part quality. Three suggestions are made with regards to thermal control during processing for improved quality. First, the part may require annealing in the mold to erase previous system "memory." Second, the part should be slow cooled through the polymer crystallization process in order to minimize frozen in residual strains from anisotropic cooling. Thirdly, the part should be heated slowly past the polymer melting process to minimize thermal gradients and warping from anisotropic heating effects.

CONCLUSIONS

Significant dimensional changes, representing 6 linear percent expansion and shrinkage, occur during heating of the ceramic/EVA system. Expansion occurs at low temperatures before weight loss begins, and can be quantitatively explained in terms of the thermal expansion behavior of the constituents and the crystallization or melting of the semicrystalline polymer. Irreversible anisotropic displacements occur during the first heating cycle due to relaxation of molding strains. The irreversible displacements can be reduced by annealing at 125°C for times comparable to the viscoelastic relaxation time, which was determined to be 8 minutes for this ceramic/EVA system. Temperature and mineral oil content did not significantly effect this relaxation time.

Significant shrinkage occurs during the early stages the of degradation of EVA. This shrinkage is quantitatively accounted for with volume losses resulting from removal of the EVA.. Shrinkage continues as weight loss proceeds and stops only at the point the ceramic particles contact one another. Further weight loss results in pore development. Total displacement behavior is the sum of the shrinkage from weight loss plus the expansion from thermal expansion of the individual components, and can be quantitatively predicted for simple or multi-step heating schedules.

Due to thermal expansion of the polymer, the volume fraction of ceramic powder was shown to significantly change during the heating of the specimen.

ACKNOWLEDGMENT

This research was supported by the Defense Advanced Research Projects Agency and the Office of Naval Research through grant N00014-94-1-0278.

TABLE I Selected properties of the ethylene co-vinyl acetate polymer

Melt index: 0.7 dg/min	M_n = 100,000	M_w = 250,000
T_g = -20°C	T_m = 84°C	Density = 0.941 g/cm^3
Percent Crystalline = 10%	FORMULA $-[(CH_2-CH_2)_x-(CH-CH_2)_y-]_n$ $\lvert$ $O-C-CH_3$ $\lVert$ O	vinyl acetate (VA) content = 18wt%

TABLE II Composition of specimens examined in rheometer for relaxation times

Specimen	Ceramic (volume percent)	EVA (volume percent)	Mineral Oil (volume percent)
1	0	100	0
2	51	49	0
3	51	43	6
4	51	37	12
5	51	31	18

TABLE III Summary of DSC data

Type	Number of Samples	Specimen Composition (ceramic/EVA/Mineral Oil) (volume percent)	T_m (°C)	T_c (°C)	ΔH_f (J/g of EVA)	% xtal.
I	3	0/100/0	90	74	29.9±0.8	10.4±0.3
II	3	0/75/25	88	72	29.4±0.6	10.3±0.2
III	3	54.5/39.5/6	85	71	17.9±1.4	6.2±0.5
IV	9	51/49/0	85	72	19.5±0.4	6.8±0.1

TABLE IV Volume fraction of phases

Phase	SiC/EVA/HMO 51/49/0	SiC/EVA/HMO 54.5/39.5/6
α-SiC	47.3	50.5
α-Al_2O_3	2.5	2.7
Y_2O_3	1.2	1.3
PE (Amorphous EVA)	39.0	31.4
PVA (Amorphous EVA)	6.7	5.4
Crystalline EVA	3.3	2.7
Mineral Oil	None	6

REFERENCES

1. T. ZHANG and J.R.G. EVANS, J. Mater. Sci. Lett., **9** (1990) 672.
2. M.J. EDIRISINGHE and J.R.G. EVANS, J. Mater. Sci., **22** (1987) 2267.
3. M. TRUNEC and J. CIHLAR, J. Eur. Ceram. Soc., **17** (1997) 203.
4. J.K. WRIGHT, M.J. EDIRISINGHE, J.G. ZHANG and J.R.G. EVANS, J. Am. Ceram. Soc., **73** [9] (1990) 2653.
5. M.A. MULLA and V.D. KRSTIC, J. Mater. Sci., **29** (1994) 934.
6. DO-HYEONG KIM and CHONG HEE KIM, J. Am. Ceram. Soc., **73** [5] (1990) 1431.
7. K.E. HRDINA in "Phenomena During Thermal Removal of Binders" (University of Michigan , Ph. D. Thesis, 1997) p.186.
8. K. E. HRDINA, J.W. HALLORAN, M. KAVIANY, and A.M. OLIVEIRA, J.Mater. Sci., In press.
9. U.S. RAMELOW, and N. GUIDRY, Microchemical J., **50,** (1994) 57.
10. N.E. CLOUGH, R.W. RICHARDS, and T.IBRAHIM, Polymers **35** [5] (1994) 1044.
11. O. OLABISI, L.M. ROBESON and M.T. SHAW in "Polymer-Polymer Miscibility" (Academic Press, NY, 1979) p. 182.
12.Y.S. LIPATOV in "Physical Chemistry of Filled Polymers" (Intl. Polymer Sci. and Tech. Mono. No. 2, translated from Russian by R.J. Moseley, 1979) p. 41.
13. R.H. PERRY, D.W. GREEN, and J.O. MALONEY in "Perry's Chemical Engineering Handbook," 6th Edition (McGraw-Hill, NY, 1984) p. 9.
14. W.F. BLAND and R.L. DAVIDSON in "Petroleum Processing Handbook" (Mc-Graw-Hill Book Company, NY, 1967) p. 12.
15. Penrico Product Bulletin for Drakeol 35 Heavy Mineral Oil.
16. L.E. NIELSEN, and R.F. LANDEL in "Mechanical Properties of Polymers and Composites," 2nd edition (Marcel Dekker, NY, 1994) pg's. 109, 384 and 64.
17. N.J. MILLS, J. of Appl. Poly. Sci., **15** (1971) 2791.
18. N.S. ENIKOLOPYAN, M.L. FRIDMAN, I.O. STALNOVA, V.L. POPOV in Filled Polymers I Science and Technology, ed. N.S.Enikolopyan (Springer-Verlag, NY, 1990) p.1.
19. J.L. KOENIG, C-H CHIANG, 503-516, The Role of the Polymeric Matrix in the Processing and Structural Properties of composite Materials, edited by J. Seferis, and L. Nicolais (Plenum Press, New York, 1983) p. 503.
20. G.W. SCHERER, Ceram. Trans., **12**, in Ceramic Powder Science III, ed. G.L. Messing and H.H. Technische (Am. Ceram. Soc., Inc., Ohio, 1990) p. 561.
21 G.W. SCHERER, J. Am. Ceram. Soc., **73** [1] (1990) 3.

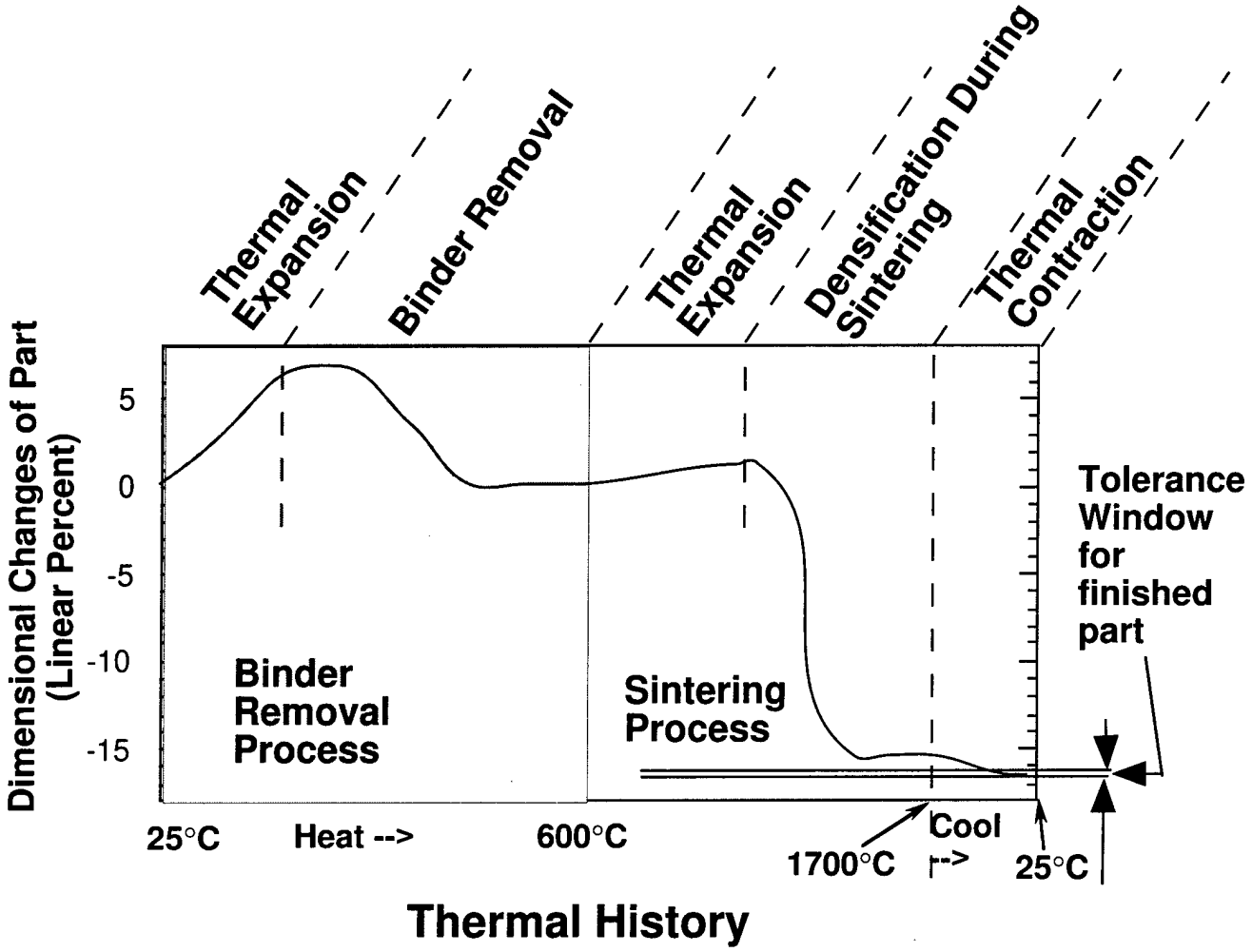

Fig. 1.
K. Hrdina & J. Halloran

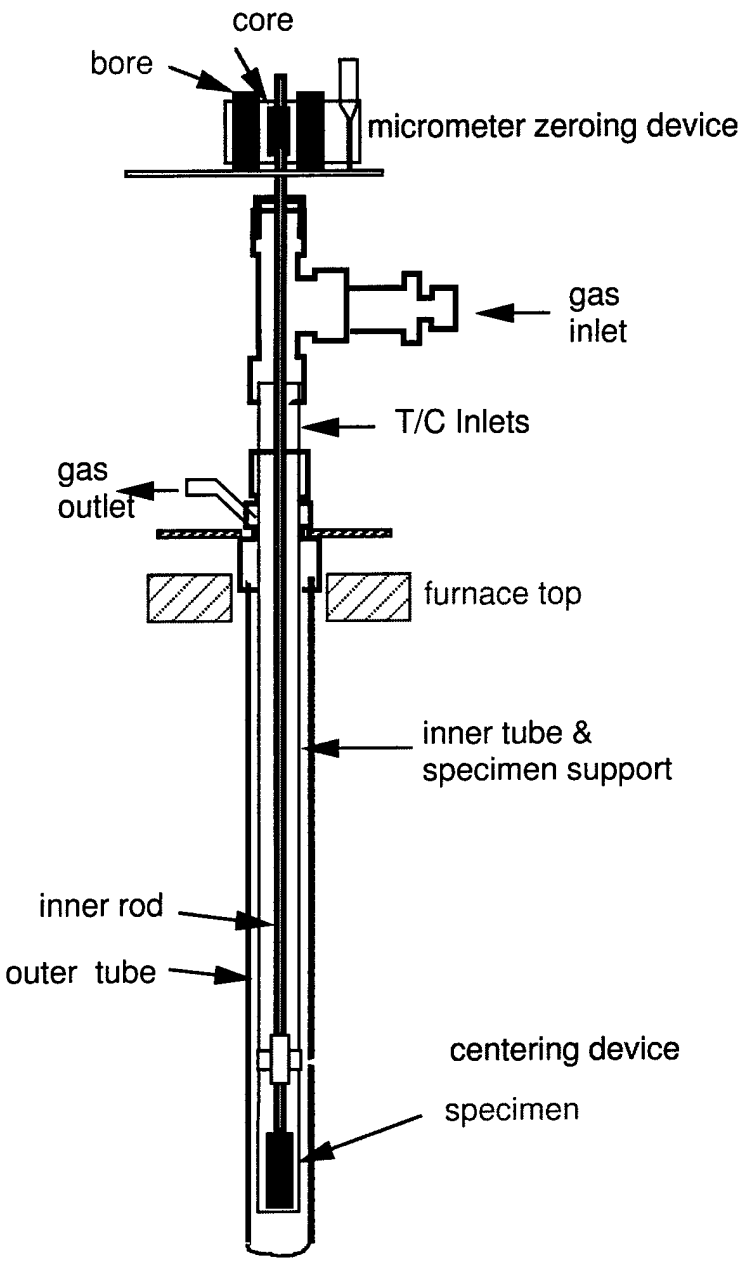

Fig. 2
K. Hrdina & J. Halloran

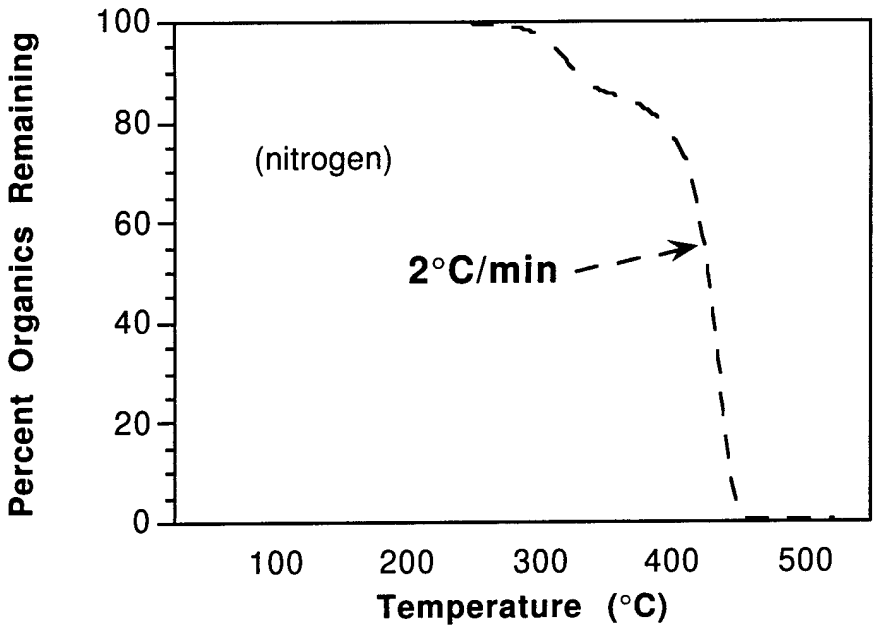

Fig. 3.

K.Hrdina & J. Halloran

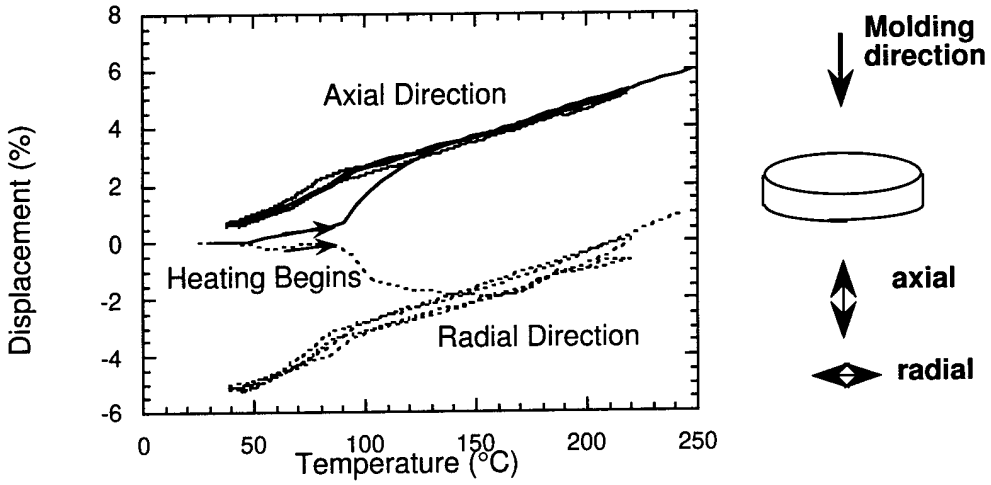

Fig. 4.
K. Hrdina & J. Halloran

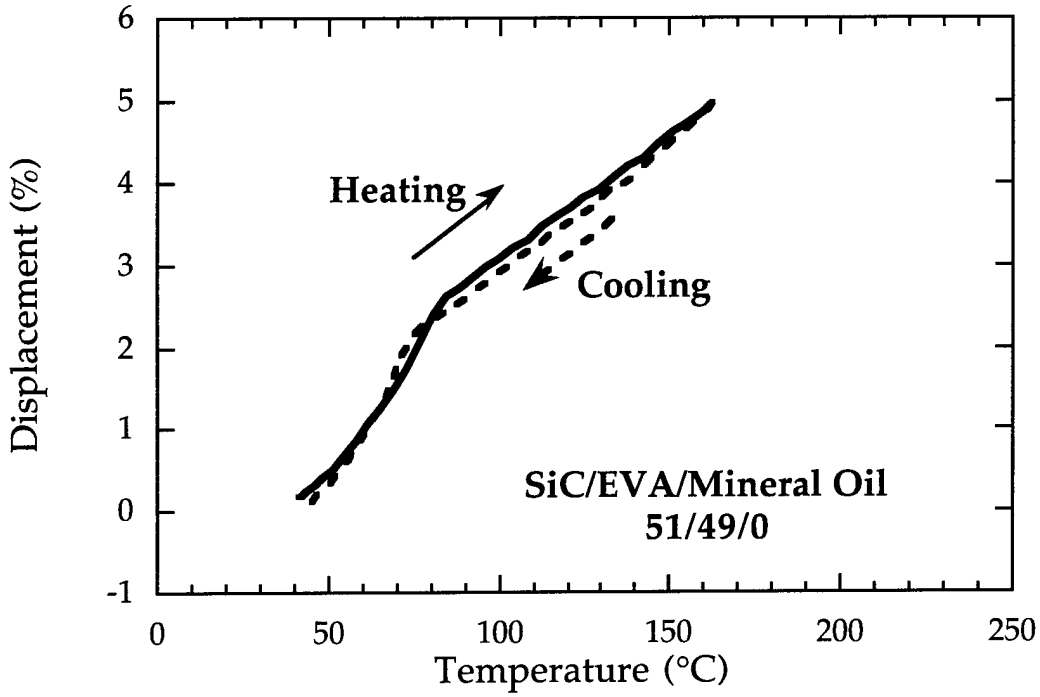

Fig. 5
K. Hrdina & J. Halloran

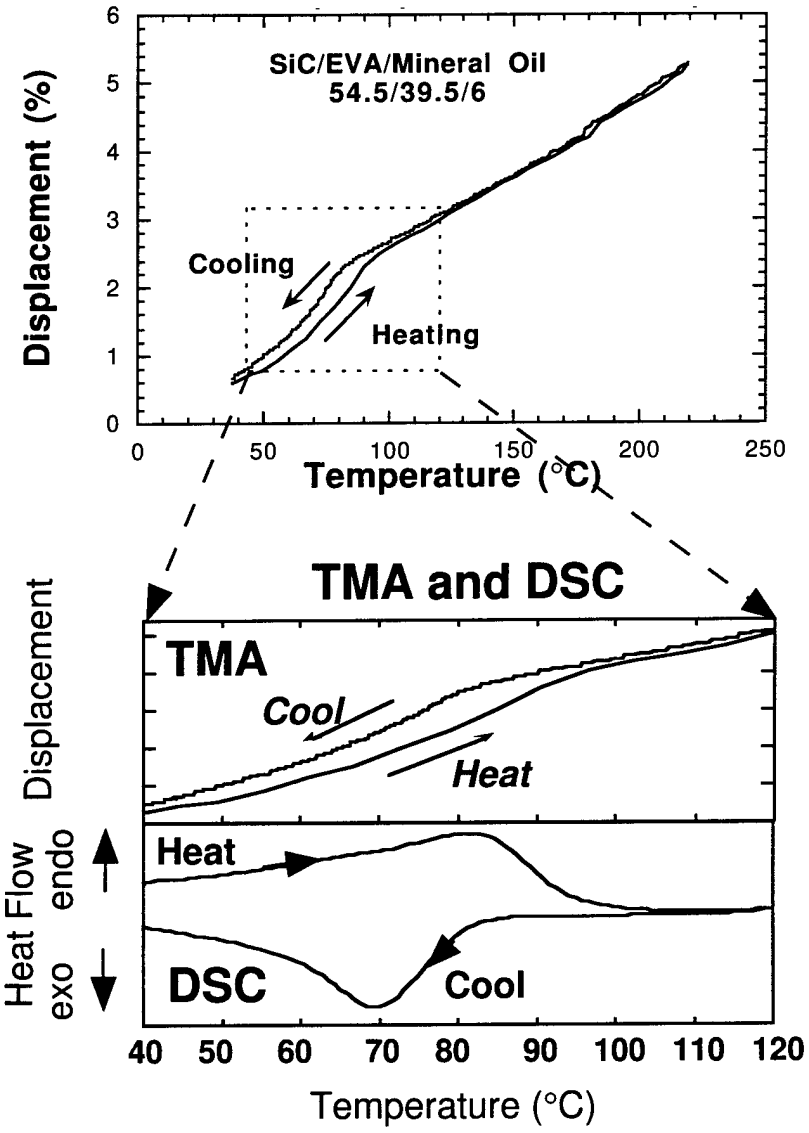

Fig. 6a & 6b
K. Hrdina & J. Halloran

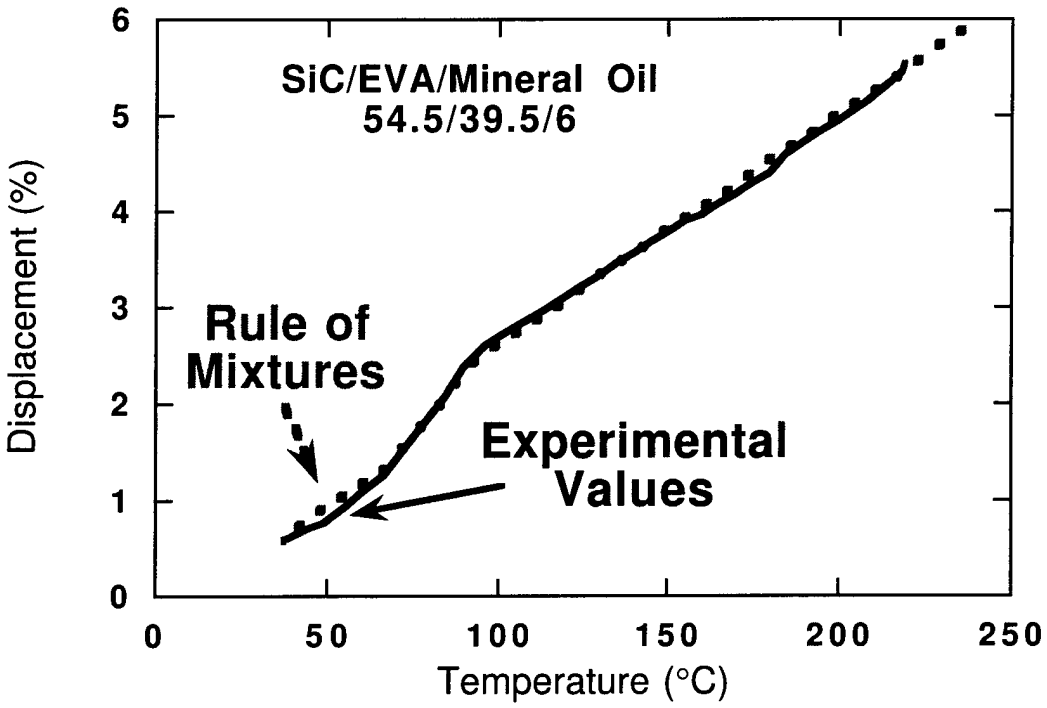

Fig. 7
K. Hrdina & J. Halloran

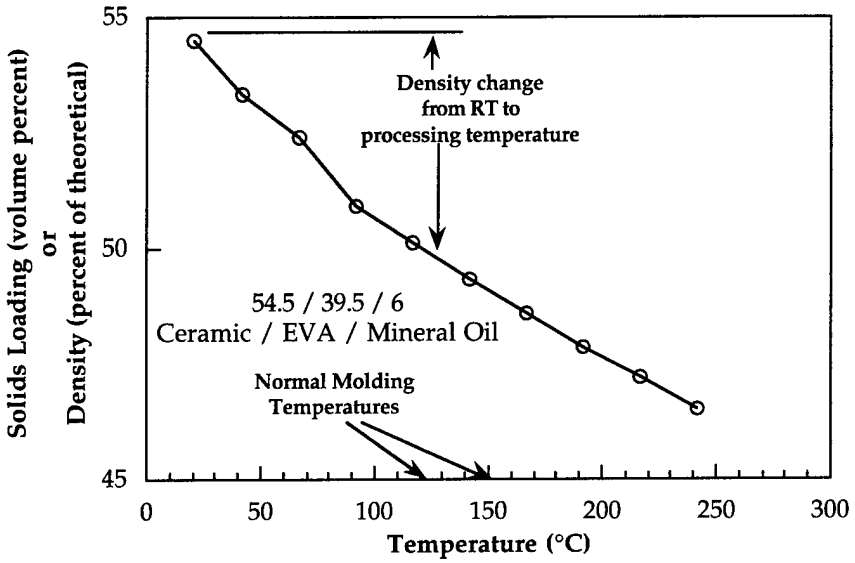

Fig. 8
K. Hrdina & J. Halloran

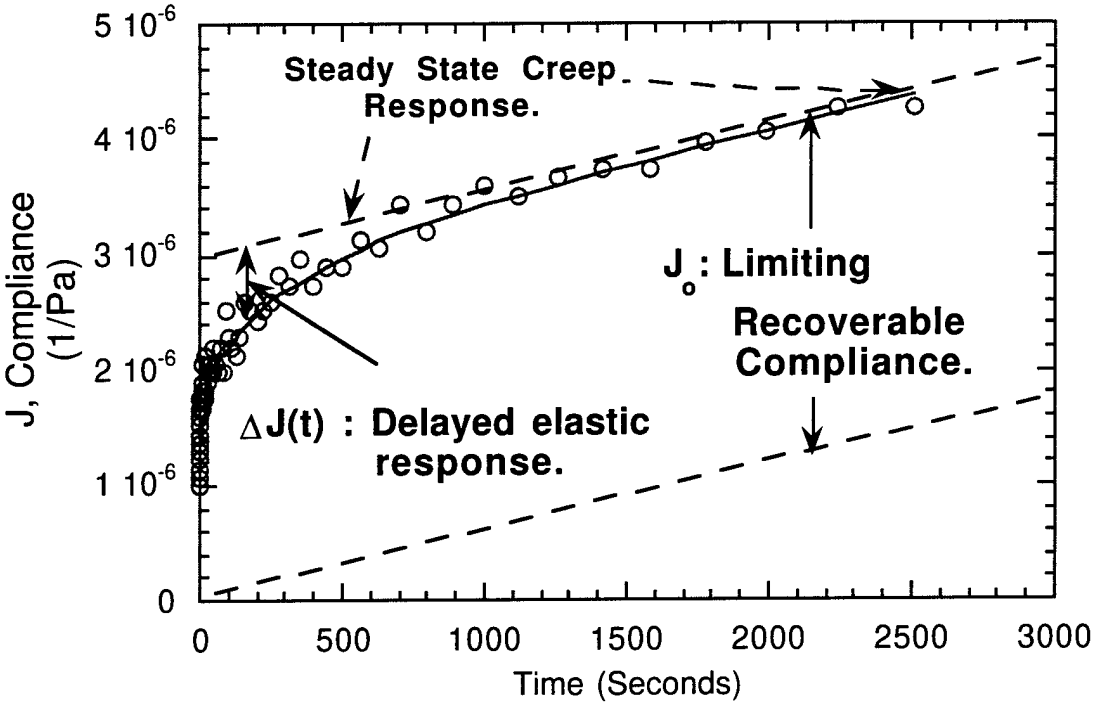

Fig. 9
K. Hrdina & J. Halloran

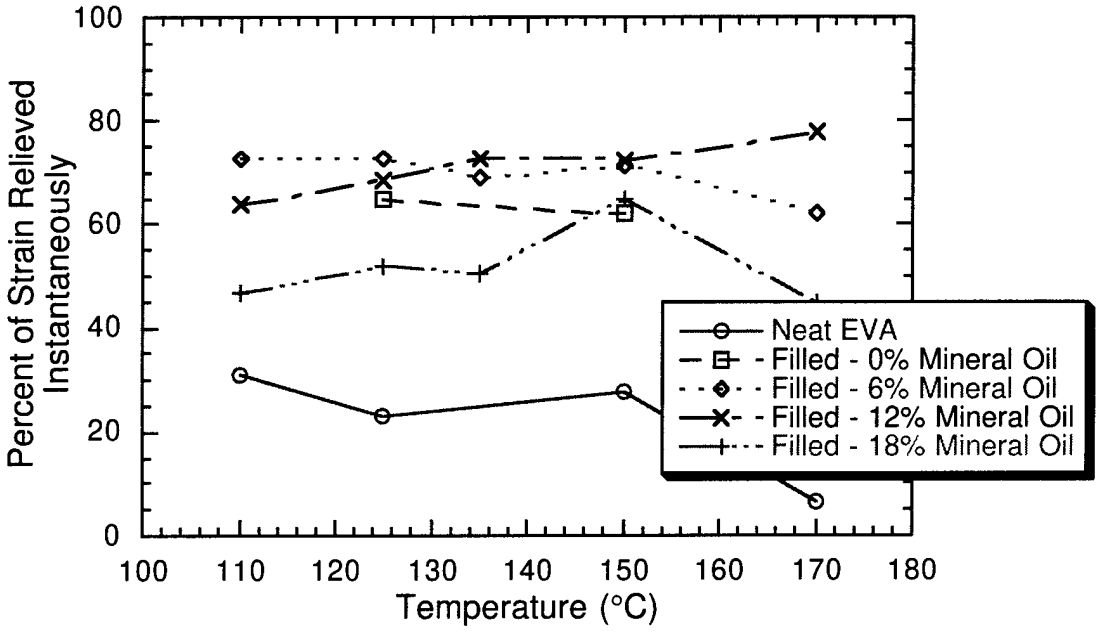

Fig. 10
K. Hrdina & J. Halloran

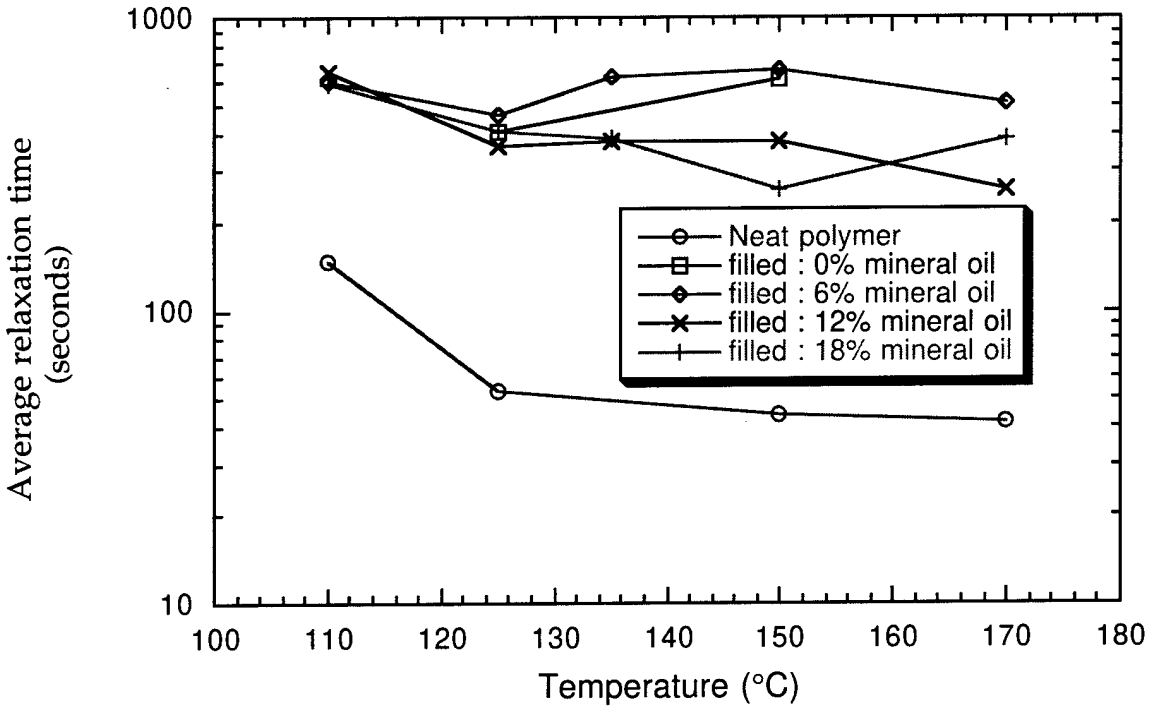

Fig. 11
K. Hrdina & J. Halloran

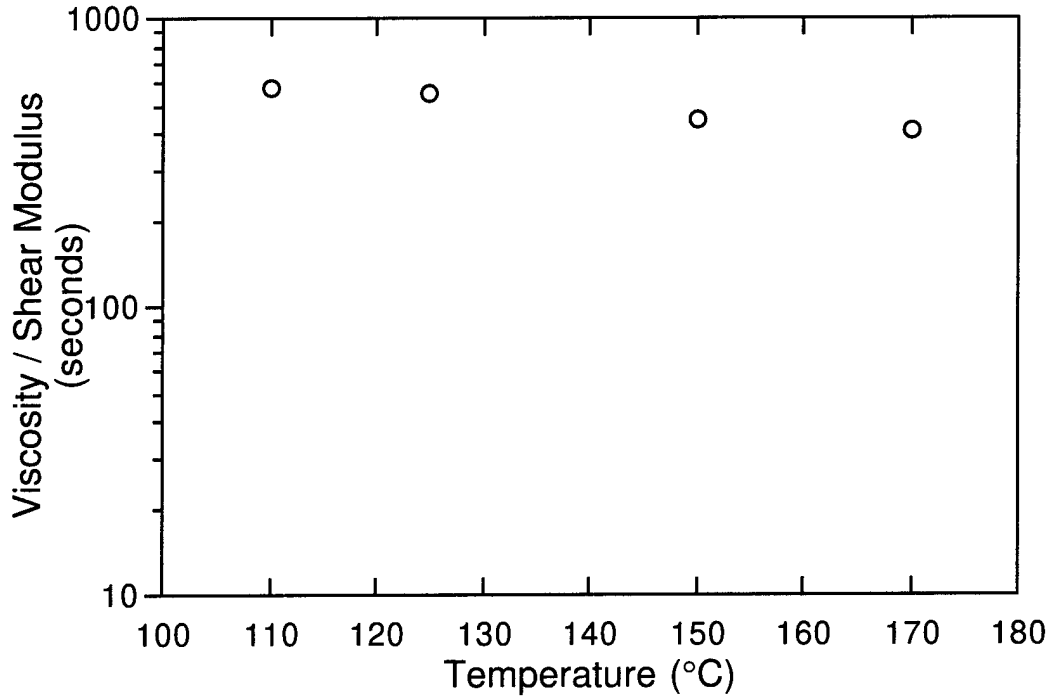

Fig. 12
K. Hrdina & J. Halloran

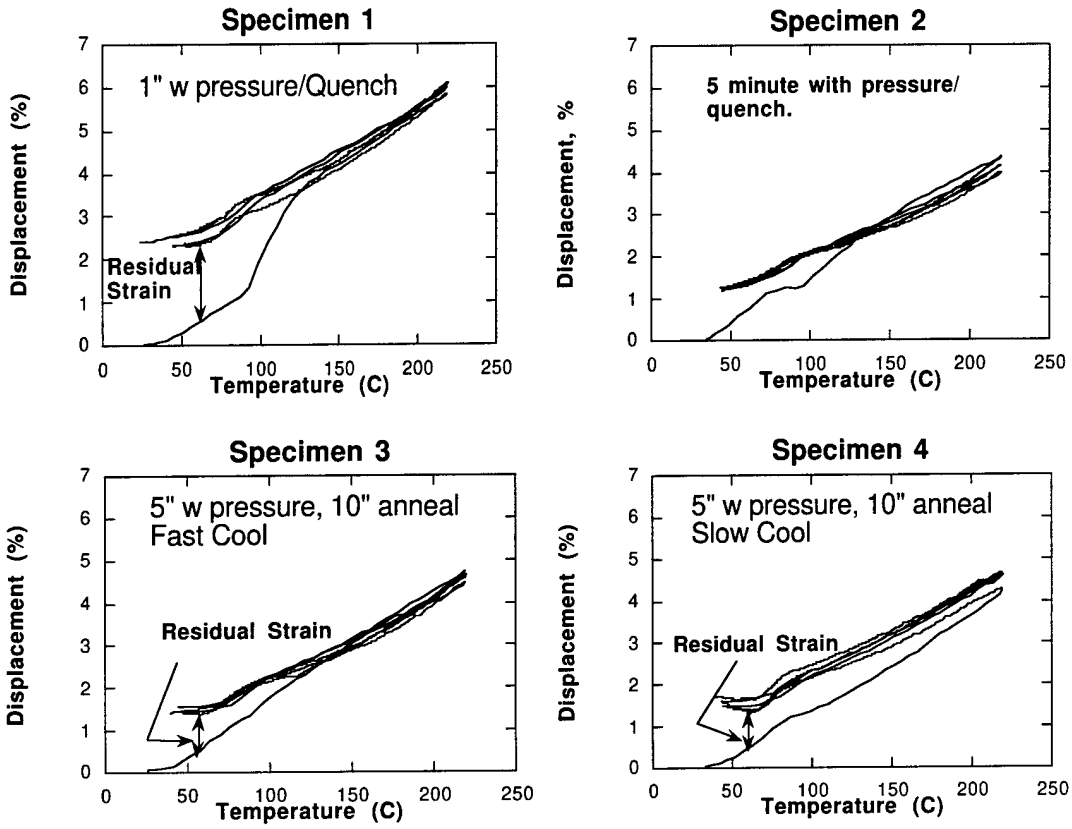

Fig. 13
K. Hrdina & J. Halloran

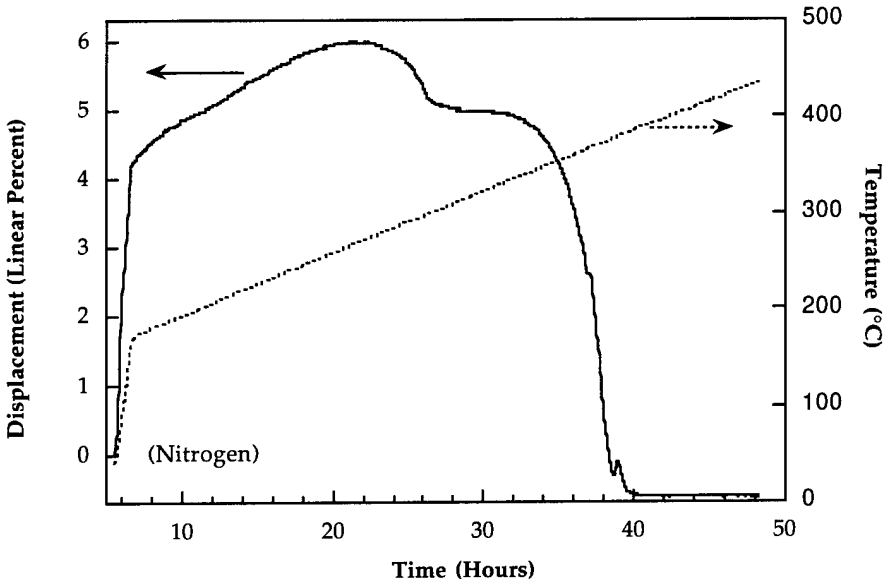

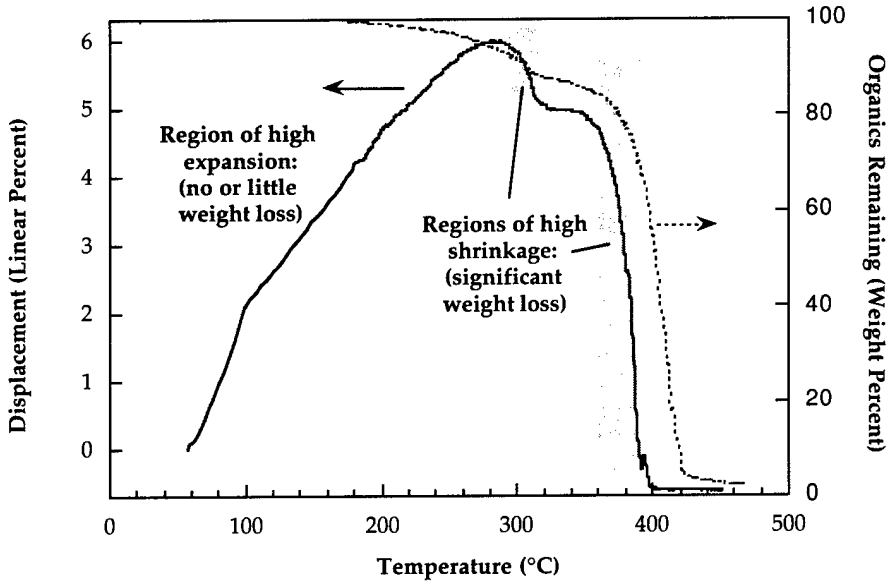

Fig. 14 a & b
K. Hrdina & J. Halloran

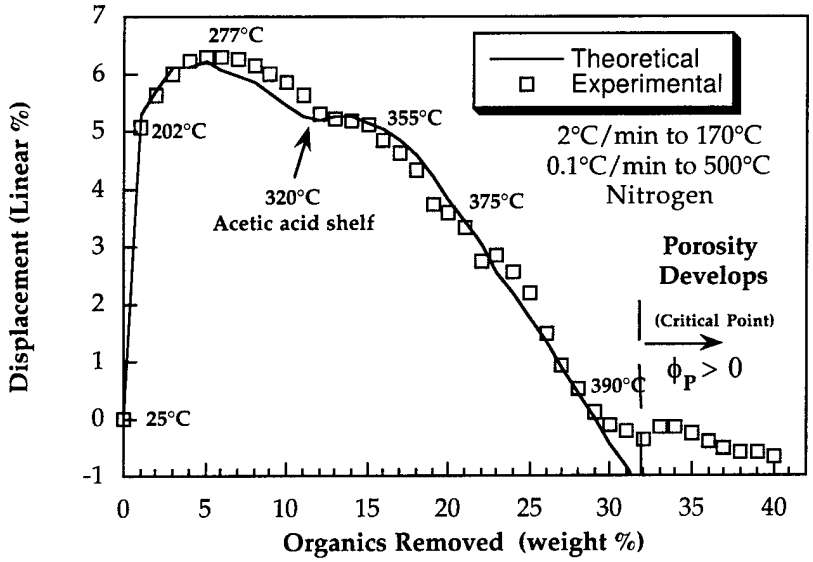

Fig. 15
K. Hrdina & J. Halloran

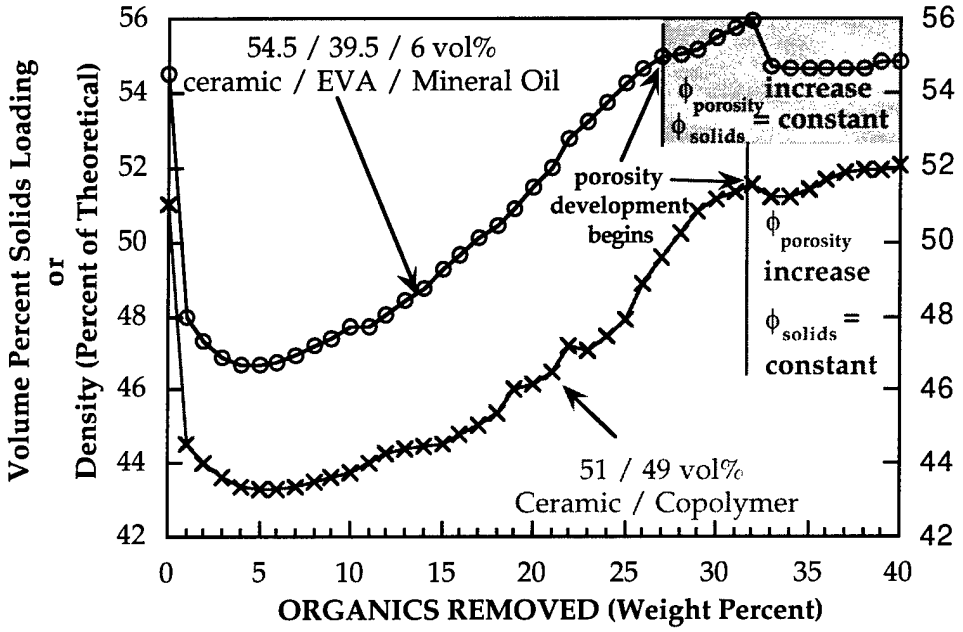

Fig. 16
K. Hrdina & J. Halloran

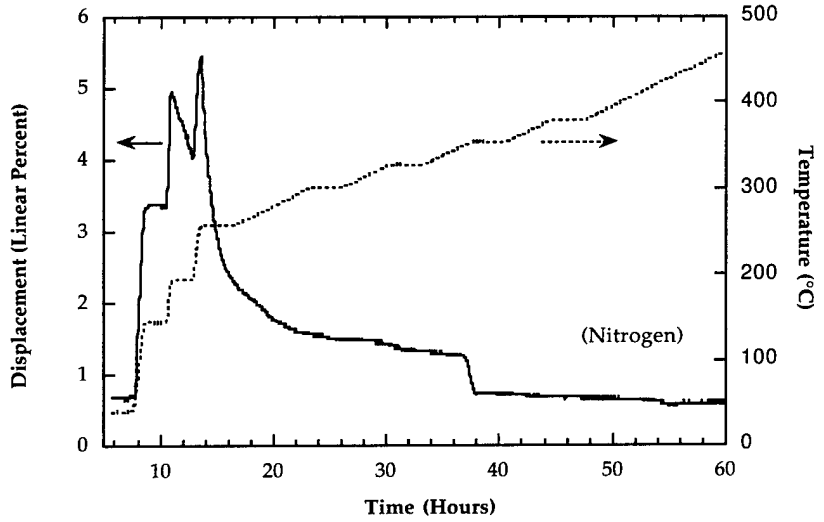

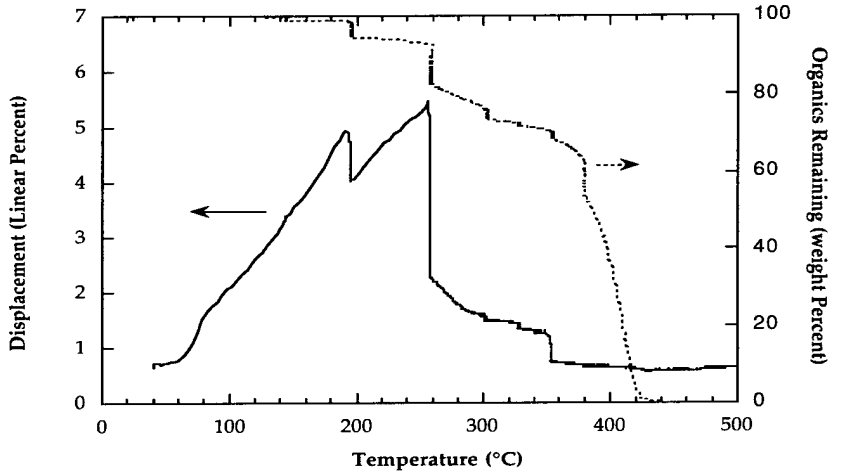

Fig. 17a & B
K. Hrdina & J. Halloran

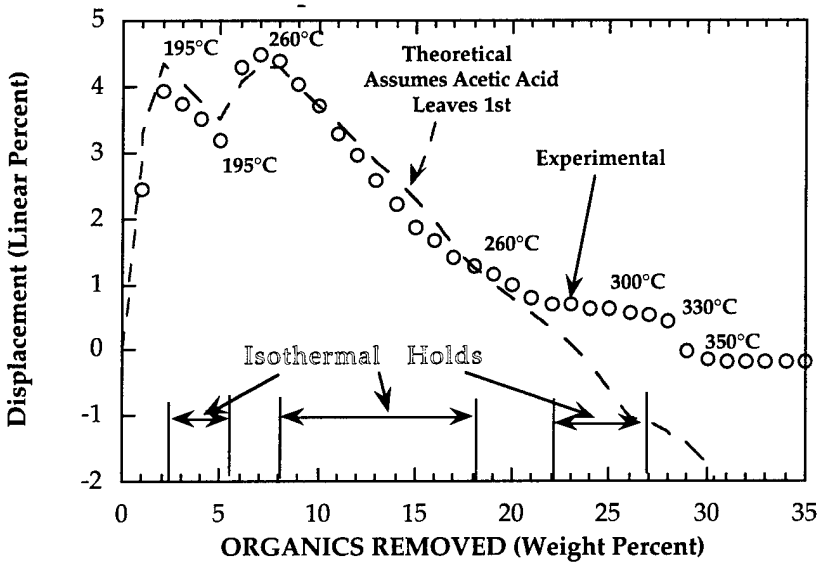

Fig. 18.
K. Hrdina & J. Halloran

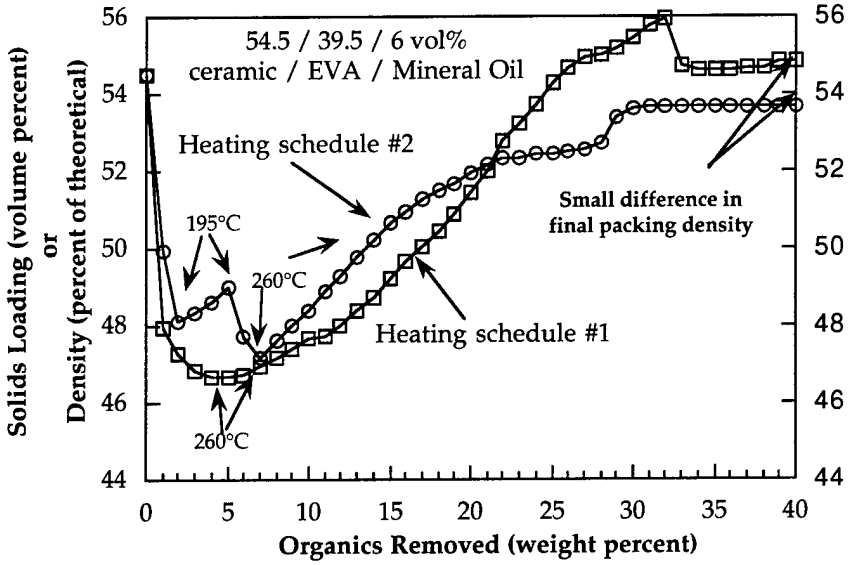

Fig. 19.
K. Hrdina & J. Halloran

Chemistry of Removal of Ethylene Vinyl Acetate Binders

Kenneth E. Hrdina, John W. Halloran, Massoud Kaviany, and Amir Oliveira
University of Michigan

ABSTRACT

The research presented herein has focused on debinding of an ethylene copolymer from a SiC based molded ceramic green body within an inert atmosphere. Upon heating the pure polymer undergoes a two stage thermal degradation process. In the first stage, acetic acid is the only degradation product formed. The effect of the introduction of high surface area powder on the chemistry and kinetics of this first stage reaction was examined. The effluents were captured and analyzed in a gas chromatograph / mass spectrometer. The product of the reaction was not altered by introduction of the ceramic powder. However, the kinetics of the reaction were altered. The kinetics of the reaction were determined with use of a TGA.

The mechanism of mass transport during binder removal was determined by monitoring dimensional changes during binder removal. It was found that one unit volume of shrinkage corresponded with one unit volume of binder removed, indicating that no porosity developed. The escaping acetic acid effluents must diffuse through the liquid polymer filled pores to escape. Bloating was observed in certain conditions and was attributed to the concentration of acetic acid exceeding a critical value, resulting in bubbling.

keywords: chemistry, kinetics, removal

1. Introduction

The process of binder removal from moldable ceramic materials is quite complicated. Most systems contain multicomponent species which themselves may degrade during thermal decomposition to additional species. Often it is not clear which species are involved and what rate they are being generated and removed. This paper examines binder removal in a simplified system which contains submicron SiC powder and an ethylene vinyl acetate (EVA) copolymer. The initial product of EVA degradation is exclusively acetic acid, a single component and well known organic species with an atmospheric boiling point of 118°C. EVA is not only a model system, but also a practical binder for molded components [1-3].

Others have noted that the presence of high surface area ceramic powder alters the reactions taking place in other binder systems [4-6]. This paper specifically investigates the effect that high surface area ceramic powder has on the chemistry and kinetics of the first stage degradation reaction of EVA. It is during initial stages of binder removal, when organic species must diffuse through the polymer filled pores, that most binder burnout problems arise [7-12]. This is the region which is studied in this paper.

Large dimensional changes were also observed to occur during the thermal degradation process of this filled systems. These dimensional changes which can lead to warping, creeping and cracking in the system were extensively reported in another paper [13]. A third paper examines in detail the type of defects observed in the present system within the initial stages of binder removal [14]. Finally, the initial stages of binder removal are modeled for the present system in another set of papers [15,16].

Ethylene vinyl acetate is a random co-polymer of ethylene and vinyl acetate. Upon heating in nitrogen, it first undergoes a side group elimination reaction [17] which generates acetic acid and leaves a double bond in the polymer chain, so the remaining polymer can be considered poly ethylene co-polyacetylene. This process can be represented by:

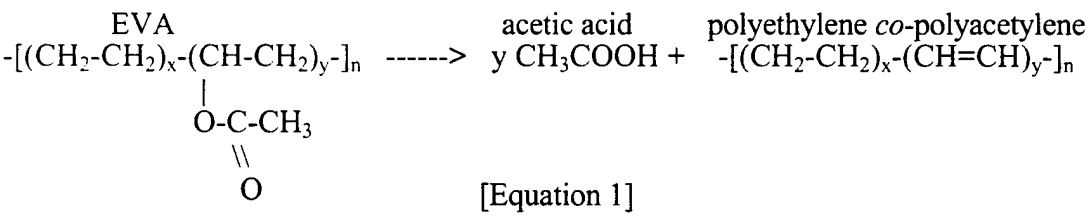

[Equation 1]

This reaction is well characterized by thermogravimetric analysis [TGA], and can be used to quantitatively analyze the vinyl acetate content of EVA [18,19]. Fig. 1 compares

the TGA degradation behavior of polyethylene to that of EVA [18]. The vinyl acetate is eliminated at a much lower temperature than the temperature at which polyethylene begins to degrade. This results in what was termed the "acetic acid shelf" in the TGA plot of EVA degradation. At this stage, the remaining polymer is a copolymer of polyethylene *co*-polyacetylene. The second stage degradation reaction was not studied in depth, but the stability of the remaining polymer up to temperatures of around 400°C (depending on heating rate) was noted.

The critical stage of binder removal in this as well as other filled polymer systems [20,21] is during initial weight loss. It is at this time, in the current system, that bloating is often observed. Therefore, the primary focus of this paper is on this first stage of binder removal that occurs during the acetic acid elimination reaction. In the present system, the copolymer has 18 wt% vinyl acetate content, which, upon initial polymer degradation, will result in 12.5% of the co-polymer's weight converting to acetic acid. Note that the degradation reactions take place at temperatures above the boiling point of acetic acid. The amount converted assumes that the reaction is unaltered by the presence of the ceramic powder. A large portion of this paper explores the effect of the ceramic powder on the degradation process. This includes how the presence of the powder has altered the reaction rate and also examines if the ceramic powder has altered the product of the reaction. To do this, effluents were collected and then analyzed within a gas chromatograph (GC) and mass spectrometer (MS).

2. Experimental procedures

2.1. Composition and processing

The polymer-ceramic powder composition is reported as a nominal room temperature volume percent, based on the room temperature densities of the components. The compositions are 51 volume percent ceramic powder + 49 volume percent co-polymer for the ceramic/EVA system, or 54.5 vol.% ceramic + 39.5 vol. % EVA + 6 vol. % mineral oil for the systems containing mineral oil. The EVA copolymer[1] has 18 weight percent vinyl acetate content. Table I lists some of the properties of the EVA polymer. The ceramic powder is prepared by ball milling using alumina grinding media, an isopropyl alcohol slurry composed of silicon carbide[2], 6 weight percent aluminum oxide[3] and 4 weight percent yttrium oxide[4] for 24 hours. The alumina / yttria ratio used is a eutectic

[1] ELVAX 470, DuPont.
[2] B-SiC, H.C. Starck Grade B 10; SA = 14-17 m^2/g, mps = 0.75 um.
[3] Malakoff Industries, Inc., RC-HP DBM; SA=7-8 m^2/g, mps = 0.55 um.
[4] Johnson Matthey, mps = 1-2 um.

composition [mp = 1760°C] which facilitates liquid phase sintering of SiC [22-25].The ceramic powders were mixed by ball milling in isopropanol for 24 hours, using alumina grinding media, followed by drying. Blending of the powder with the resin is done in a heated shear mixer[5] with roller blades. The EVA resin is added first and melted under shear at 130°C at a constant speed of 60 RPM. The ceramic powder is added in small increments of mixing for 1-2 minutes. The increased shear, upon adding the powder, increases mixing temperatures to 150-160°C. The mineral oil[6], if used, is added next.

The binder uniformity in a batched material and between batches of material was checked by the random selection of four specimens from two separate batches of material. The percent of binder in each material was determined by TGA analysis. These results indicate no significant differences between binder content within a batch of material or between batches. The molding process may lead to preferential binder distribution if the polymer phase preferentially flows or is extruded away from high pressure regions leaving behind a powder rich phase [26,27]. The disc-shaped specimens were compression molded at 27 MPa (4000 psi) and 120°C in a uniaxial mold. TGA analysis on molded specimens revealed no difference in the binder distribution throughout the specimen indicating that molding did not lead to any preferential binder distribution for this system.

2.2. Displacement and GC/MS measurements

Dimensional changes were measured in a thermomechanical analyzer [TMA] built specifically for studying the binder removal process from moldable green ware [13]. The same instrument was modified to collect effluents during thermal degradation of the binder system. A schematic of the instrument is shown in Fig. 2. The specimen rests on a platform at the bottom of an inner fused silica tube which is vertically oriented. A fused silica rod, rests on top of a porous fused silica plate which in turn, rests on the specimen. The porous fused silica glass with pore sizes of 90-150 μm is used to distribute the load that the rod places on the specimen and still allows unimpeded binder removal. A typical nominal pressure of 1.4 kPa rests on the specimen during each test. The LVDT core and bore reside on a fused silica support above the furnace. Elaborate cooling means were used to thermally isolate the specimen from the LVDT core system to localize all dimensional changes to that of the specimen alone. A plus or minus 1 μm change was noted during heating a blank from room temperature to 500°C.

---

[5] C.W. Brabender Instruments, Inc., PL 2000 Plasti-Corder with Roller Blade Mixing Heads.
[6] Heavy Mineral Oil, Mallinckrodt, Paraffin Oil, sp. = 0.881.

Normal displacement measurements were made with nitrogen gas flowing through the inner tube down to the specimen and then up through the annulus between the inner and outer tube to the exhaust port. Alternatively, gas effluents were collected during binder removal through the modification of the existing TMA instrument. In this instrument, a 4.5 g polymer filled specimen (51/49 ceramic / EVA) was placed on a platform at the bottom of an inner fused silica tube which is vertically oriented. The specimen was next heated at 2°C/min to 315°C with helium gas flowing past the specimen and into a liquid nitrogen cooled condensing chamber. The condensed effluents were later analyzed in a GC/MS[7]. Helium gas was used to minimize reactions in the gas phase and as a carrier gas through the liquid nitrogen trap. Once the sample had been collected, the liquid nitrogen trap containing the condensed effluents was removed and allowed to warm to room temperature while sealed with parafilm® to reduce contamination. GC/MS micro-liter samples were then taken from the condensed liquid in the container and injected into the GC/MS port.

Differential Thermal Analysis [DTA][8] was utilized to examine the endothermic/exothermic nature of the degradation reactions. The specimens were heated at 10°C/min under a flowing nitrogen atmosphere and used an alumina reference. An 8 mg sample was used for the neat EVA and an 18 mg sample was used for the 51/49 ceramic powder / EVA specimen.

A molded specimen 9 mm x 25 mm x 50 mm was heated in a nitrogen atmosphere to a temperature of 315°C for the purpose of partially removing the binder and then furnace cooled to room temperature. The specimen was heated according to a schedule used by a collaborating company that was found to produce defect-free parts. The specimen was heated from room temperature to 145°C at 1°C/min, from 145°C to 250°C at 0.033°C/min, and finally, from 250°C to 315°C at 0.067°C/min. The partially burned out specimen was sectioned using a slow speed saw[9]. The binder distribution was then determined with a TGA[2].

2.3. Kinetic measurements

Two different thermogravimetric analysis [TGA] instruments were employed. The first TGA[10], utilized small (10-30 mg) samples to study the degradation reaction kinetics of both the neat EVA and the EVA in the presence of the powder. The specimens were

---

[7]Hewlett Packard 5890.
[8]TA Instruments 1600 DTA.
[9]Buehler Isomet
2 TA Instruments
[10]TA Instruments Hi-Res TGA 2950.

placed in a platinum pan and heated at constant heating rate to determine the reaction kinetics. The second TGA[11] utilized larger specimens in which mass transport was rate limiting.

Directly measuring the EVA elimination reaction while in the presence of the ceramic is desirable. However, no direct observations were readily accessible. An estimate of the generation rate of acetic acid within the filled system was obtained by TGA weight loss data on small 25 mg size samples at constant heating rates of 1,2,4,8, and 16°C/min. In this study, kinetics were determined with the assumption that the rate of weight loss as measured by the TGA on small 25 mg specimens was equal to the rate of generation of acetic acid. This assumes that no storage or accumulation of the formed acetic acid takes place within the small 25 mg specimens. Additionally, the small 25 mg samples were cut into smaller size pieces to further reduce the transport path.

It was further assumed that the rate of acetic acid generation in the 25 mg samples corresponded with the rate at which the elimination reaction proceeded in the larger 0.5 g to 8 g specimens. Fig. 3 elaborates on this point. For example, the 25 mg sample shown in Fig. 3 was found to lose 4% of the organics weight at 300°C. The bulky 2 g sample was found to lose only 2.5% of its organics at 300°C. The rest of the acetic acid formed from the remaining 1.5% organic conversion was accumulated or stored within the sample.

3. Results and discussion

3.1. Reaction products

The specimen that was placed in the TMA for effluent collection had lost 5% (0.05g) of the organic content while heating to 315°C and then cooling. This region is clearly in regime I, the regime where only acetic acid should be formed. This is also under the 12.5% expected if total acetic acid elimination was to occur. The GC and MS results of the effluents collected are shown in Fig.'s 4a and 4b respectively. The GC results show one major peak. This indicates that only one reaction product is being formed. The mass spectrometer results shown in 4b reveal that the molecular weight of this peak is 60 which is the molecular weight of acetic acid. It appears, therefore, that the ceramic powder has not altered the product of this first stage elimination reaction. Acetic acid is still the only product of the initial stage degradation reaction.

3.2. Reaction kinetics

[11] TGA-171, ATI-CAHN microbalance.

3.2.1. TGA and DTA

The combined TGA and DTA results for the neat and filled polymer are shown in Fig.'s 5a and 5b respectively. A comparison of the TGA results for neat verses filled EVA shown in these Fig.'s reveals a difference in the first stage reaction rate for the two specimens. Neat EVA shows a clear acetic acid shelf and the filled polymer shows a more gradual weight loss process during the initial stage degradation behavior. It appears that the reaction process has been slightly altered. Section 3.2.2. will examine the kinetics in more detail.

The character of the DTA traces of the neat and filled EVA polymer shown in Fig.'s 5a and 5b are similar. In each case, three distinct endothermic peaks are seen. The endothermic peaks at 88°C and 86°C for the neat and filled polymer respectively correspond to the melting of the polymer crystals. DSC measurements were previously reported and quantitatively identified the area of the neat polymer at 29.5 J/g polymer and that of the filled polymer at 19.5 J/g polymer [13,28].

The endothermic peaks at 349°C and 375°C for the neat and filled polymer respectively correspond to the first stage elimination reaction. The peak for the neat polymer is more defined in shape while that of the filled polymer appears as a shallow trough. The high surface area ceramic filler has extended the region over which the first stage reaction proceeds so that the clearly defined acetic acid shelf in the neat polymer is not clear for this filled specimen.

The second region of weight loss, i.e., the region in which the last 88% of the binder is removed, begins with predominantly endothermic reactions and ends with predominantly exothermic reactions. For both neat and filled EVA, the last endothermic reactions increase up to the point at which only 30 to 40% of the polymer is remaining. This is attributed to chain scission and evaporation. Then, heat evolution appears to occur and accelerate until all the mass is gone. This might be evidence of carbon - carbon bond or cyclic ring formation occurring along with chain scission [29]. However, no carbon residue was measured or noted in the case of the neat polymer which might have substantiated carbon-carbon bond formation.

3.2.2. Altered kinetics

Several methods of kinetic analysis that use TGA weight loss data are presented in the literature. These methods include the isothermal temperature method [30-32], the variable heating rate method [31,33], and the method used in this research, the constant

heating rate method [31,34]. In the case of EVA degradation, the following kinetic equation is applied [31,33]:

(2) $d\alpha/dt = Ag(\alpha)\exp(-E/kT)$

where: α = Mass fraction remaining.
t = time.
A = Pre-exponent (frequency factor).
E = Activation energy.
$g(\alpha) = (1-\alpha)^n$ for EVA system.
n = Reaction order.

Table II lists results from the literature for application of this equation for regions I & II for the neat polymer only. Equation 2 provides a good description of the experimental behavior for neat EVA.

The kinetics for decomposition in region II were not of interest in this paper other than for observation that the rate of decomposition in the neat and filled specimens appeared to be the same for region II. However, it should be noted that within the literature, Equation 2 was also applied to region II and found to fit. The actual physical interpretation of the fit becomes hazy since many decomposition reactants and products are taking place in region II instead of one elimination reaction process.

The TGA results are summarized for the various heating rates in Fig. 6 for the filled EVA polymer. Faster heating rates shift the weight loss to higher temperatures.

3.2.2a Activation energy

The Flynn-Wall method was used for the determination of activation energy at various percentage levels of conversion for both the neat and filled EVA systems [31] . This is accomplished by application of the natural log of both sides of Equation 2 such that:

(3) $\ln(d\alpha/dt)_\alpha = \ln(A) + \ln[g(\alpha)] - E/kT$

A plot of $\ln(d\alpha/dt)$ verses 1/T for various constant levels of conversion should then yield a straight line with slope of -E/k.

Within the present system, the weight percent of organics that converts to acetic acid is calculated to be 12.5%. Therefore, the activation energy for the region I reaction should be the same from 0 to close to 12% conversion. Fig. 7a [31] and 7b compares the

data of Nam and Seferis to the presently utilized neat EVA system. Note that the EVA by Nam and Seferis had 30% acetic acid compared to 12.5% for our system. Note that the activation energy is constant with the percent conversion in each case, indicating an activated reaction process. Note also that the activation energy of 178 kJ/mole obtained in the present system matches the 163-186 kJ/mole activation energy in the literature.

The same Flynn-Wall plot for the filled system appears in Fig. 7c. The activation energy is still constant with the percent conversion indicating that the reaction still follows an activated process. However, the powder appears to have lowered the activation energy from 178 kJ/mole for the neat polymer to 150 kJ/mole for the filled polymer. The reason for this change is not known at this time.

3.2.2b Reaction order

A method used by Day, Cooney, and Wiles [32] was used for determination of the reaction order as per Equation 2 with $g(\alpha) = (1-\alpha)^n$. This was done at various temperatures for the region I reaction. For this method, the natural log of Equation 2 is taken such that:

$$(4) \qquad \ln(d\alpha/dt)_T = \ln(A) + n\ln(1-\alpha)_T - E/kT$$

Plots of $\ln(d\alpha/dt)$ vs. $\ln(1-\alpha)$ at constant temperatures result in straight lines whose slope is the reaction order. The resultant reaction order at various temperatures are plotted in Fig. 8 for both the neat and the filled polymer. The reaction order for the neat polymer appears constant with temperature indicating that Equation 2 with $g(\alpha) = (1-\alpha)^n$ appears to describe the reaction. The reaction order of 0.8 for the neat polymer is not much different from the reaction order of 0.9-1.2 from the literature [33]. The reason for this small difference is considered to be within experimental variations.

As seen in Fig. 8, the reaction order for the filled system is not constant with temperature so that $g(\alpha)$ does not equal $(1-\alpha)^n$ in this case. The ceramic powder has appeared to alter the kinetics so that the reaction cannot be simply described since $g(\alpha) \neq (1-\alpha)^n$. The more detailed kinetic analysis required to better describe the kinetics was beyond the scope of this research and is the subject of future investigation.

3.2.2c Powder adsorbates and pre-existing degradation products

The presence of the ceramic powder has not only appeared to alter the kinetics of the degradation reaction, but also has another characteristic that differentiates it from the neat polymer. Fig. 9 is an example of this distinct region at a heating rate of 2°C/min. This Fig. shows that weight loss on the order of 0.7% of the total organic content is observed at temperatures of about 100°C for the filled system. As will be shown in another paper [15,16,28], this low temperature region is partially responsible for some of the bloating behavior.

Further investigation indicate that some, but not all may be attributed to adsorbates on the ceramic powder. For detailed results, see Hrdina [28]. However, it is noted that the kinetics of the filled system, even with correction for adsorbents, are still different from that of the neat EVA. The altered kinetics are not from adsorbents on the powder. The reason for the altered kinetics was not identified. Catalytic effects in which the reaction process is speeded up might explain the weight loss at lower temperatures in the ceramic filled system. However, it does not explain why the final stages of the region I reaction are not also accelerated, but are delayed.

The altered kinetics might be explained by another possibility. Perhaps, some decomposition of the EVA polymer took place during prior shear mixing in the plasticorder. The mixing in the plasticorder is at high shear rates and at temperatures close to the decomposition temperature of neat EVA (150°C to 170°C). It is suspected that the mechanical and thermal energy input may have been enough to cause some partial decomposition of EVA which resulted in some "precharging" of the filled polymer with acetic acid. The kinetics may have been altered as a result of the presence of pre-existing acetic acid.

It should also be noted that the polymer used in this study contains 0.02 to 0.1 wt% BHT (Butylated hydroxytoluene) which is an antioxidant added by the manufacturer with a boiling point of 265°C [35]. This quantity of material does not account for the 0.7% organic weight change observed.

3.3. Mechanism of mass transport

The mechanism for binder removal presented in this paper is based on the premise that molecular species originate from throughout the specimen and then diffuse through the liquid polymer to the surface where they then evaporate. These two conditions must be met by the system. The first, that the diffusing species originate from throughout the specimen, is dealt with here. The second condition, that the species are diffusing through the liquid polymer, is examined in the following section.

The molecular species leaving the filled EVA system is acetic acid generated from the vinyl acetate portion of the copolymer. A sectioning experiment was undertaken to infer if the degradation was occurring uniformly through the thickness of the material. A specimen was heated to 300°C, which would result in approximately 10 weight percent removal. The sample was sectioned into 0.5 mm slices, as shown in Fig. 10, and the amount of polymer in each slice was determined by TGA. The TGA data indicated that each slice had experienced an average of 10.8 weight percent loss, uniformly through the thickness.

It should also be noted that the uniform distribution of binder seen in Fig. 10 leads to the conclusion that acetic acid has not appreciably accumulated within the sample. The transport of acetic acid out of the sample was apparently fast enough to remove the generated acetic acid from the sample for this particular heating schedule.

We infer that the acetic acid is transported by diffusion through the liquid polymer during the early stages of the binder removal because there is no open porosity in the samples until more than 30 wt% of the binder has been removed. We report elsewhere [13] that these samples undergo 6% linear shrinkage and remain fully saturated as the first 30% of the binder is removed. Generation of volatile species takes place within the entire system as a result of thermal decomposition of the polymer. The generated species then diffuse through the liquid polymer phase to the surface of the specimen where they are removed by evaporation. Samples containing mineral oil have the same mechanism of mass transport in this filled polymer system.

3.4. Phenomena of bloating

The predominant defects that show up in this system appear to start as an internal crack, and then develop into bloats. They are a result of the acetic acid exceeding a critical concentration. A typical example of a defect observed in the present system is shown in Fig. 11. This particular specimen is 3 mm thick and was heated at 2°C/min to 270°C and cooled. Two rather large bubbles are shown that appear near the center of the specimen. Duplicate specimens heated to 250°C at the same rate did not bloat.

It should be remembered that acetic acid is forming everywhere in the material during heating. It was also shown that acetic acid diffuses through the system to the surface. Therefore, the region of highest concentration is expected to be the specimen center which has the longest diffusion path. This is also the primary region where bloating is observed. The bloating is also associated with the initial region of weight loss. Acetic

acid was found to be the overwhelming product of the reaction in this region as was reported in Section 3.1.

Most bubbles within the filled specimens occur near the center of the specimen, but location varies somewhat from specimen to specimen and from bubble to bubble within a center. This suggests that a minimum supersaturation appears required for formation of a bubble. A more detailed examination of bubble formation is reported in [15,16].

3.5. Conclusions

The EVA co-polymer degradation process can be broken into two distinct regions. In the first region, EVA undergoes an elimination reaction that results in the evolution of acetic acid. TGA and DTA results show that the ceramic powder has altered the reaction rate. However, GC/MS results show that the ceramic powder has not altered the reaction product. Acetic acid is still the primary product. The second stage reaction loses weight in a manner similar to the degradation behavior of polyethylene.

The kinetics of degradation for neat EVA in the first region of decomposition where acetic acid is formed follows first order kinetics with an activation energy of 178 kJ/mole. The addition of the ceramic powder altered the kinetics of the reaction so that they no longer appear to follow any reaction order. The reason for the altered kinetics is not known, but "precharging" may contribute to the apparent alteration in the kinetics.

The escaping species from the filled system was shown to originate throughout the specimen. No porosity develops during initial stages of binder removal. Therefore, it is concluded that during the initial stages of binder removal, the escaping species, which in this case is acetic acid, must be diffusing through the liquid polymer filled pores to the specimen surface where it then evaporates.

Finally, bubble or crack formation occurs during heating from the acetic acid concentration exceeding a critical level.

ACKNOWLEDGMENT

This research was supported by the Defense Advanced Research Projects Agency and the Office of Naval Research through grant N00014-94-1-0278.

3.6. References

1. M. TRUNEC & J. CIHLAR, J.Eur. Ceram. Soc., **17** (1997) 203.
2. G. RENLUND and C. JOHNSON, US PATENT # 4,571,414 (1986).
3. S.J. STEDMAN, J.R.G. EVANS, and J. WOODTHORPE, Ceramics International, **16** (1990) 107.
4. W.K. SHIH, M.D. SACKS, G.W. SCHEIFFELE, Y.N. SUN., and J.W. WILLIAMS, Ceram.Trans.: Ceramic Powder Processing Science, ed. by G.L. Messing, E.R. Fuller, Jr. and H. Hausner (Am. Ceram. Soc.,Westerville, OH 1988).
5. S. MASIA, P. D. CALVERT, W.E. RHINE, and K. BOWEN, J. Mater. Sci., **24** (1989) 1907.
6.Y.N. SUN, M.D. SACKS, and J.W. WILLIAMS, Ceram.Trans.: Ceramic Powder Processing Science, ed. by G.L. Messing, E.R. Fuller, Jr. and H. Hausner (Am. Ceram. Soc., Westerville, OH 1988) p. 538.
7. P. CALVERT and M. CIMA, J. Amer. Ceram. Soc., **73** [3] (1990) 575.
8. J.R.G. EVANS, M.J. EDIRISINGHE, J.K. WRIGHT, and J. CRANK, Proc. Roy. Soc. London, A **432** (1991) 321.
9. H.M. SHAW and M.J. EDIRISINGHE, Phil. Mag., A, **72** [1] (1995) 267.
10. S.A. MATAR, J.R.G. EVANS, M.J. EDIRISINGHE, and E.H. TWIZELL, J. Mat. Res., **10** [8] (1995) 2060.
11. E.H. TWIZELL, S.A. MATAR, D.A. VOSS, and A.Q.M. KHALIQ, Int. J. Eng. Sci., **30** [3] (1992) 379.
12. S.A. MATAR, M.J. EDIRISINGHE, J. R.G. EVANS, and E.H. TWIZELL, J. Amer. Ceram. Soc., **79** [3] (1996) 749.
13. K.E. HRDINA and J.W. HALLORAN, J. Mater. Sci., In press
14. K. E. HRDINA, J.W. HALLORAN, M. KAVIANY, and A.M. OLIVEIRA, J. Mater. Sci., In press.
15. A.M. OLIVEIRA, K.E. HRDINA, M. KAVIANY, and J.W. HALLORAN, J. Mater. Sci. In press.
16. A.M. OLIVEIRA, K.E. HRDINA, M. KAVIANY, and J.W. HALLORAN, Presentation at the 1997 Nat. Heat Trans. Conf., Balt., MD, August 10-12, 1997.
17. H.H.G. JELLINEK, in Degradation of Vinyl Polymers, Chapter 2 (Academic Press, Inc., NY 1955).
18. R.J. KOOPMANS, R. VAN DER LINDEN, and E.F. VANSANT, Poly. Eng. and Sci., Mid-October, **22** [14] (1982) 878.
19. I.M.SALIN and J.C.SEFERIS, J. Appl. Poly. Sci., **47** (1993) 847.
20. I.E. PINWILL,M.J.EDIRISINGHE and M.J.BEVIS, J.Mater. Sci., **27** (1992) 4381.
21. R. GILISSEN and A. SMOLDERS, in High Tech Ceramics, ed. by P. Vincenzini(Elsevier Science, Amsterdam, Netherlands, 1987) p. 591.
22. M.A. MULLA and V.D. KRSTIC, Ceram. Bul., **70** [3] (1991) 439.
23.M.A. MULLA and V.D. KRSTIC, J. Mater. Sci., **29** (1994) 934.
24. DO-HYEONG KIM and CHONG HEE KIM, J. Amer. Ceram. Soc., **73** [5] (1990) 1431.
25. V.D. KRSTIC personnel contact October, 1994.
26. R. GERMAN, in Powder Injection Molding (Metal Powder Industry Federation, Princeton, 1990) chapter 10.
27. B.O. RHEE, M.Y. CAO, H.R. ZHANG, E. STREICHER, and C.I. CHUNG in Advanced Powder Metallurgy, Part 2, Powder Injection Molding (1991) p.43.
28. K.E. HRDINA, in Phenomena During Thermal Removal of Binders (Ph.D. Thesis, University of Michigan, May, 1997).
29. S.S. STIVALA, J. KIMURA, and S.M. GABBAY in Degradation and Stabilization of Polyolefins, edited by N.Allen, (Applied Science Publisher, NY, 1983) p.82.
30. JAE-DO NAM and J. SEFERIS, J.Poly. Sci.: Part B: Poly. Phys., **30** (1992) 455.
31. JAE-DO NAM and J. SEFERIS, J. Poly. Sci.: Part B: Poly. Phys., **29** (1991) 601.

32. M.DAY, J.D. COONEY, and D.M. WILES, Poly. Eng. and Sci., **29** [1] (1989) 19.
33. I.M. SALIN and J.C. SEFERIS, J.Appl. Poly. Sci., **47**, (1993) 847.
34. W.E. MODDEMAN, W.C. BOWLING, E.E. TIBBITTS, and R.B. WHITAKER, Poly. Eng. and Sci., **26** [21] (1986) 1469.
35. DuPont ELVAX Resin Literature, #184528E, reorder #H-44016-1, October 1, 1992.

TABLE I Selected properties of EVA 470

Melt index: 0.7 dg/min	M_n = 100,000 M_w = 250,000	T_g = -20°C T_m = 84°C
Density = 0.941 g/cm^3	FORMULA $-[(CH_2\text{-}CH_2)_x\text{-}(CH\text{-}CH_2)_y\text{-}]_n$ $O\text{-}C\text{-}CH_3$ O	Percent Crystalline = 10% vinyl acetate (VA) content = 18wt%

TABLE II Literature values for kinetics of neat EVA [33]

REGION	Log (A)	Reaction Order,n	Activation Energy, E (kJ/mole)
I	13.2	0.9-1.2	163-186
II	18.2-19.0	0.6-0.9	248-270

List of Figures

Fig. 1 Degradation of Ethylene Vinyl Acetate [EVA] compared with Low Density Polyethylene [LDPE] from Reference 17

Fig. 2 Schematic of thermomechanical analyzer [TMA] modified to collect effluents for gas chromatograph [GC] / mass spectrometry [MS]

Fig. 3 Fraction of organics remaining in sample, from thermogravimetric analysis for small 25 mg samples and large 2 g samples

Fig. 4 a) GC
b) MS

Fig. 5 a) DTA/TGA unfilled
b) DTA/TGA filled

Fig. 6 TGA of filled EVA at constant heating rates

Fig. 7 Activation energy as function of conversion for the Flynn-Wall method applied to
a) unfilled EVA (open circles - this work: filled circles - Nam & Seferis [31])
b) filled EVA

Fig. 8 Reaction order as a function of temperature for the Day, Cooney, Wiles method applied to EVA. The unfilled EVA follows first order kinetics. The filled EVA does not follow this same type of kinetic behavior

Fig. 9 TGA traces showing initial weight loss at temperatures below 100°C for filled systems at 2°C/min heating

Fig. 10 Binder distribution in partially burned out specimen showing evidence that the binder is removed from throughout the specimen

Fig. 11 Typical bloating defect observed in present system

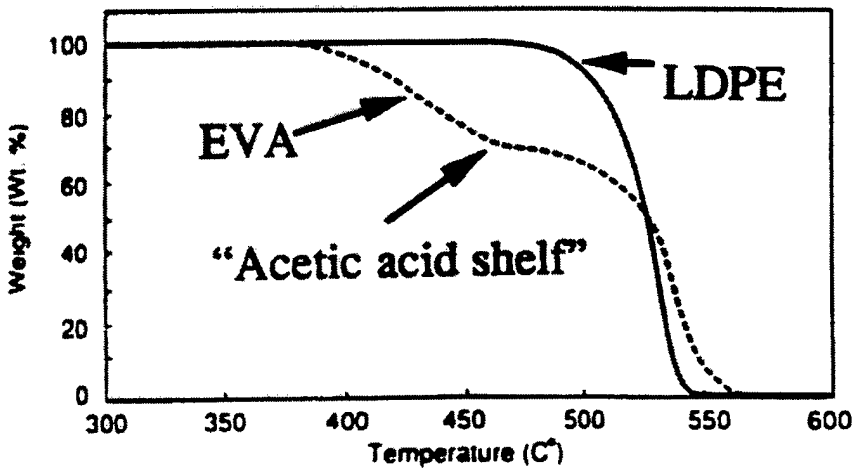

Fig. 1

Hrdina, Halloran, Kaviany & Oliveira

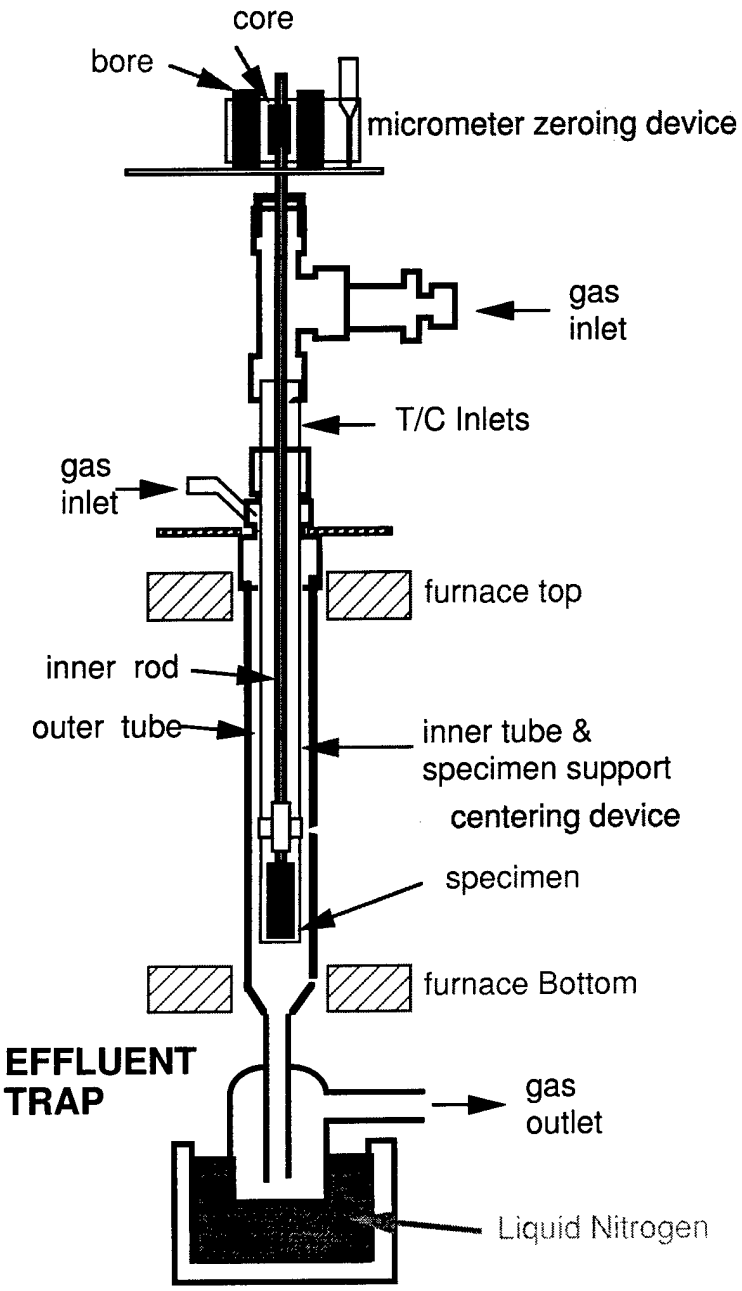

Fig 2 Hrdina, Halloran, Kaviany & Oliveira

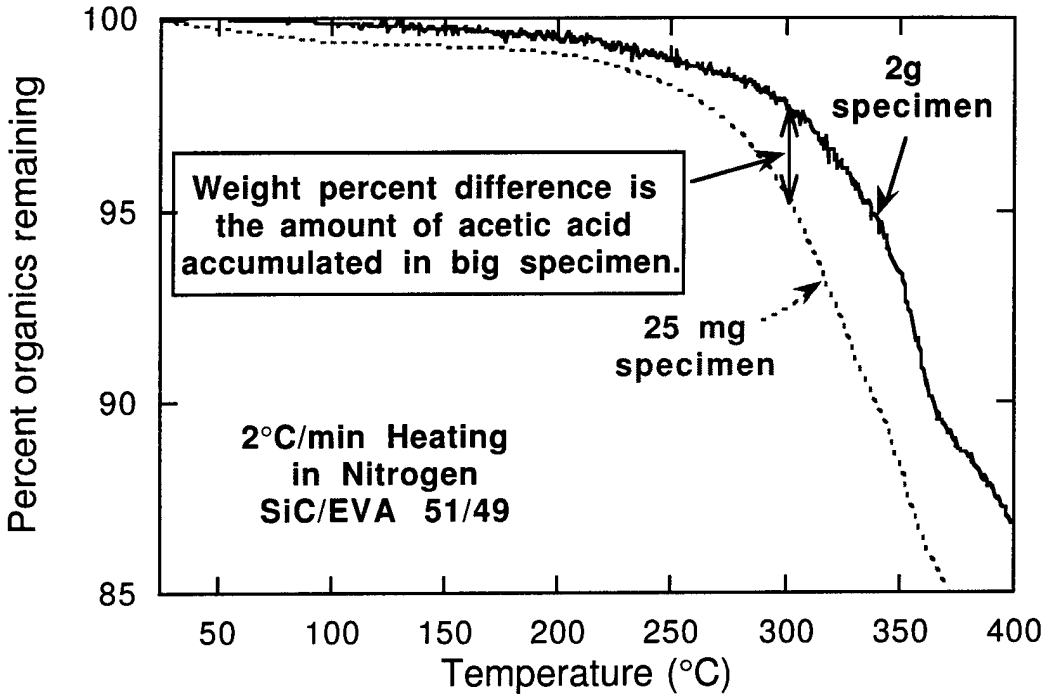

Fig 3 Hrdina, Halloran, Kaviany & Oliveira

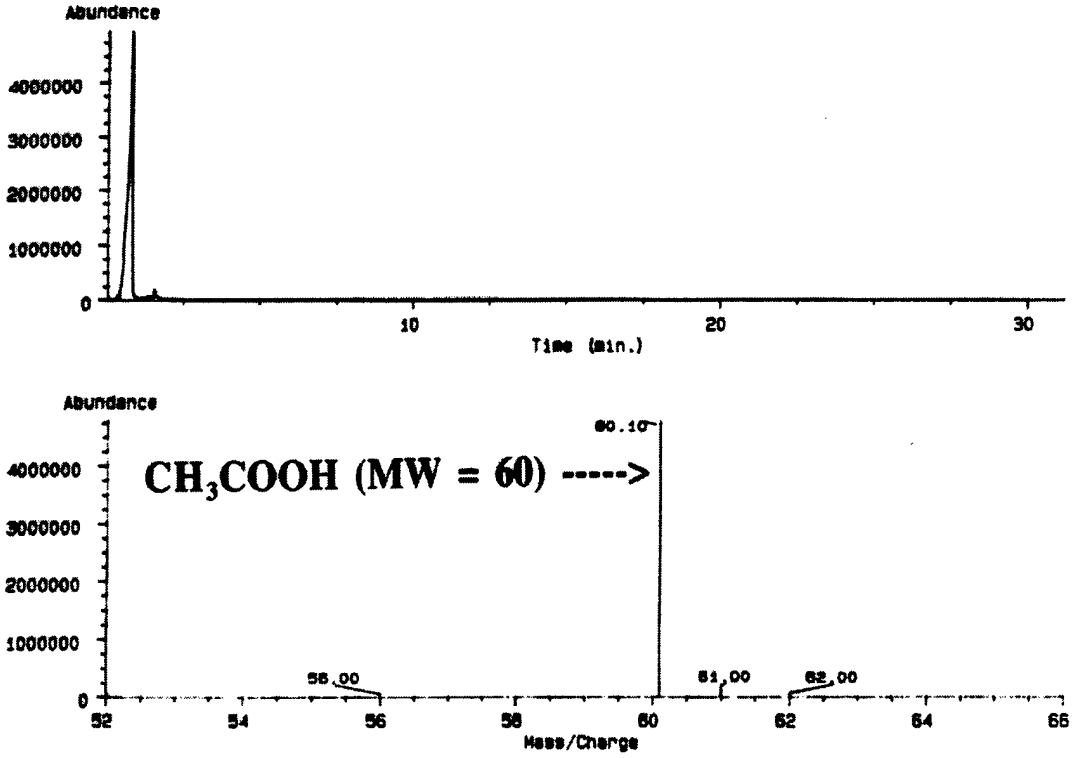

Fig 4 a & b Hrdina, Halloran, Kaviany & Oliveira

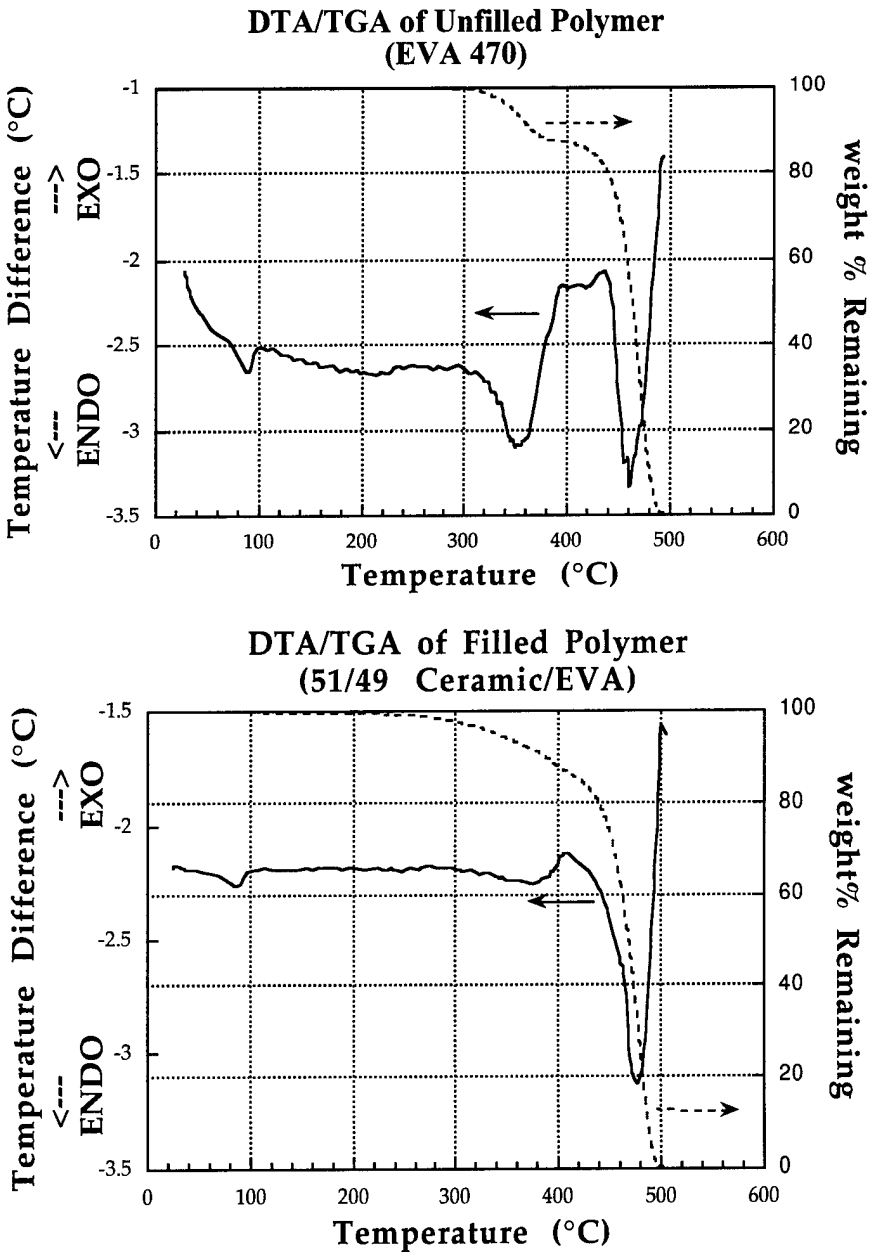

Fig 5 a & b Hrdina, Halloran, Kaviany & Oliveira

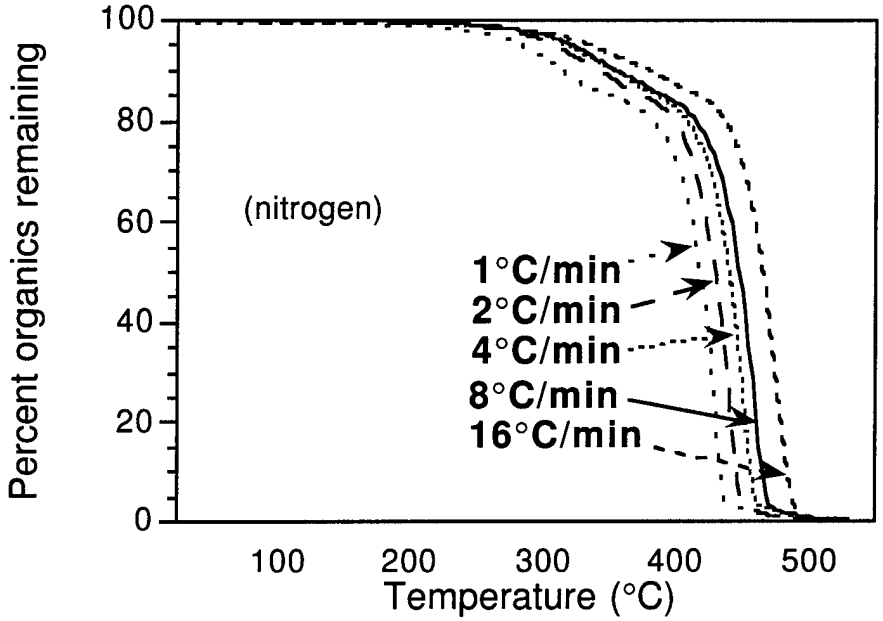

Fig 6 Hrdina, Halloran, Kaviany & Oliveira

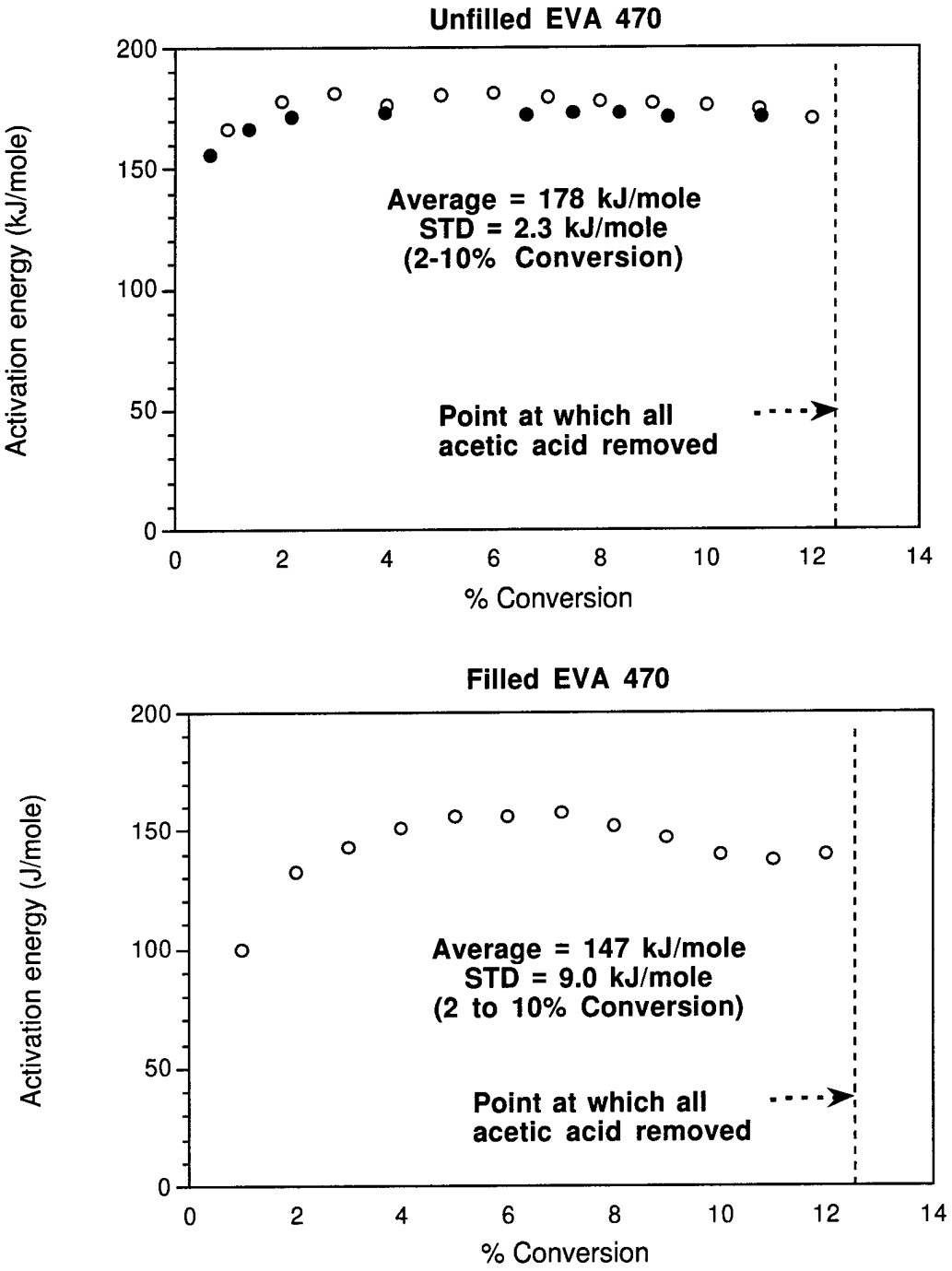

Fig 7a & b Hrdina, Halloran, Kaviany & Oliveira

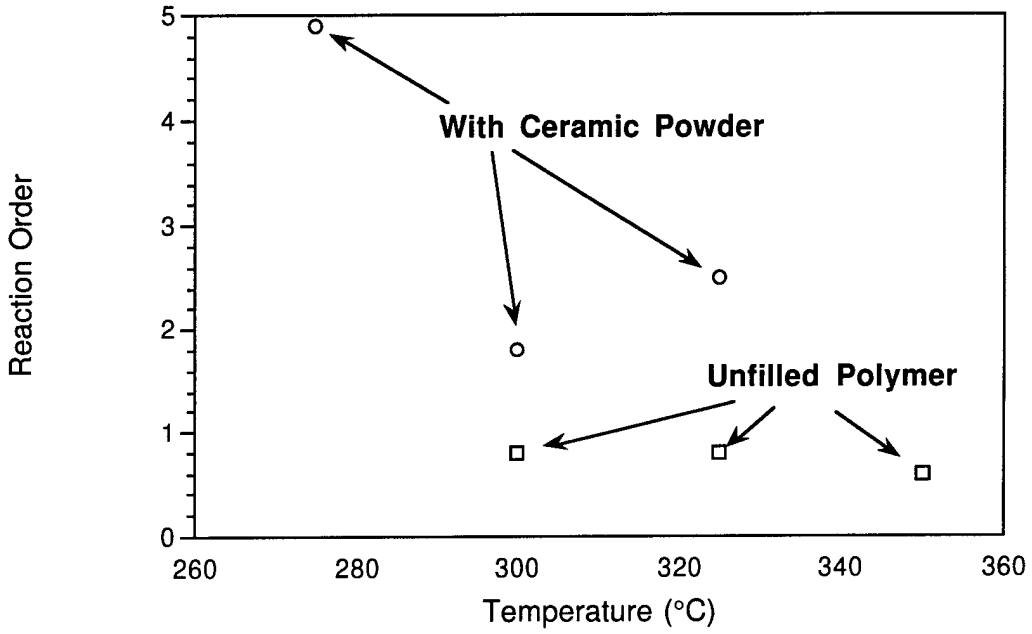

Fig 8 Hrdina, Halloran, Kaviany & Oliveira

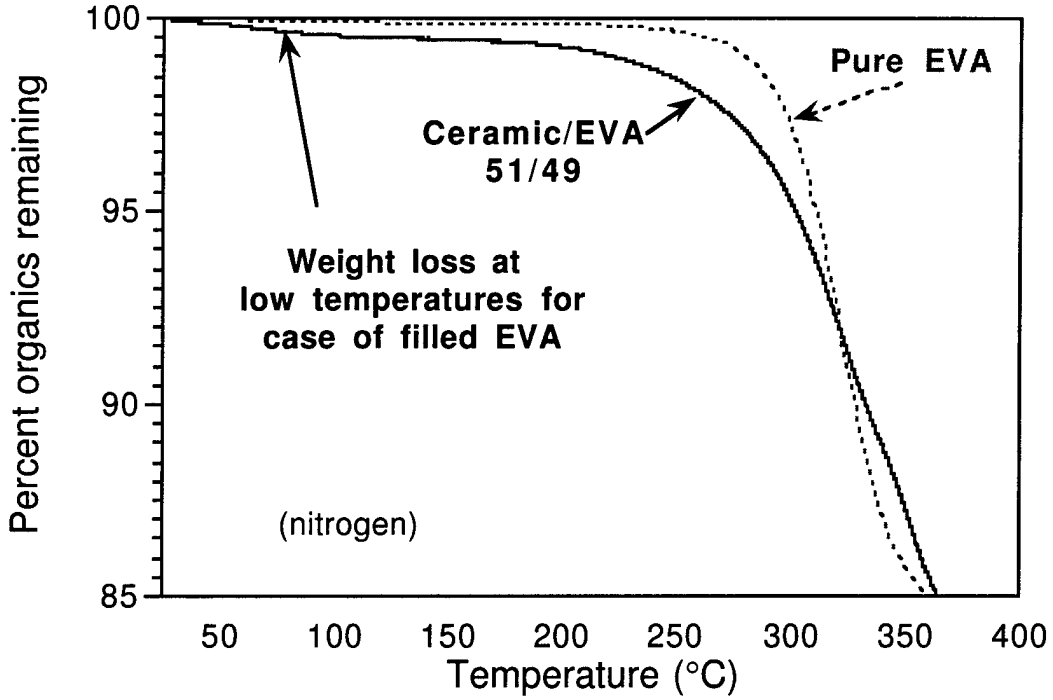

Fig 9 Hrdina, Halloran, Kaviany & Oliveira

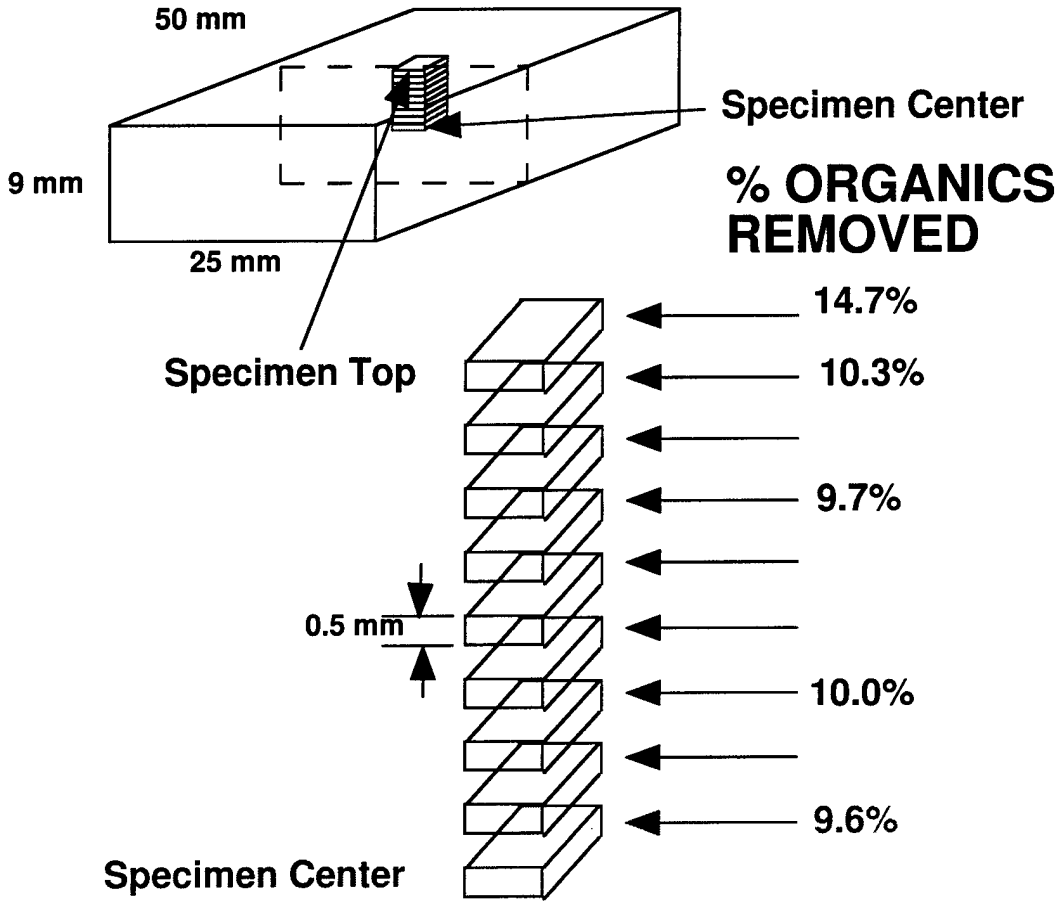

Fig 10 Hrdina, Halloran, Kaviany & Oliveira

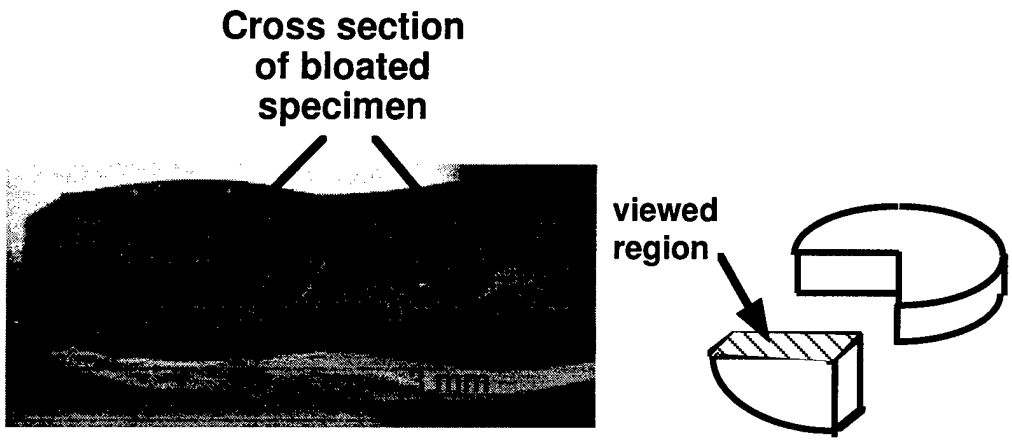

Fig 11 Hrdina, Halloran, Kaviany & Oliveira

Defect Formation During Binder Removal in Ethylene Vinyl Acetate Filled System

Kenneth E. Hrdina, John W. Halloran, Massoud Kaviany, and Amir Oliveira
University of Michigan

ABSTRACT

This paper focuses on determining the criteria for defect formation during the early stages of thermal binder removal within an ethylene vinyl acetate (EVA) polymer filled with submicron SiC ceramic powder. The only product of the early stage thermal degradation reaction of EVA within an inert atmosphere is acetic acid. This single component and well characterized organic reaction product has allowed the defect forming criteria to be definitively examined. It will be shown that bloating occurs in the early stages of binder removal as a result of pressure build-up in the specimen resulting from acetic acid formed from the thermal elimination reaction of EVA.

The first part of this paper examines defect formation occurring in the pure polymer within a hot-stage optical microscope. Bubble formation is observed in the pure polymer. Next, bloating occurring in the molded system is examined. The affect of mineral oil on bloating is also discussed as well as the effect that molding pressure has on bloating. It was found that molding pressure effects defect formation. Finally, this paper presents binder removal maps that were developed for specimens up to 8 mm thick. These bloating maps indicate the existence of two primary bloating regimes.

keywords: defect, binder, map

1. Introduction

The primary problems encountered in binder removal in filled systems typically occur in the early stages of binder removal [1-6]. It is during this stage when organic species must diffuse through polymer filled pores before they can escape. The escaping species can either be present beforehand or can be products of the degradation reaction(s) taking place. Regardless of there origin, problems such as cracking, bloating or warping may occur during binder removal. The problem of warping or poor tolerances was addressed in a previous paper [7]. This paper specifically addresses the phenomena of cracking or bloating occurring during the early stage of binder removal in an ethylene *co*-vinyl acetate (EVA) copolymer binder system that evolves a single, well known organic species, which is acetic acid. The formation of acetic acid within the system was definitively proven in a previous paper [8]. It was also shown that acetic acid is generated throughout the specimen. The rate of formation of acetic acid was also well characterized in the previous paper while in the presence of the ceramic powder. It is forming from the degradation reaction of EVA at temperatures well above its boiling point of 118°C.

A paper by Calvert and Cima [1] models a similar process. The case when a polymer decomposes to produce a volatile monomer, in this case PMMA "unzipping" to produce MMA. A bubble is assumed to form when the monomer species concentration is such that the pressure of MMA exceeds atmospheric pressure. The diffusion of the monomer through the liquid polymer is slow, three orders of magnitude slower than diffusion through the gas phase. The decomposition rate of the polymer is causing a concentration build up of monomer within the polymer. The concentration is lowered by diffusion of the monomer out of the specimen. This behavior and the defect forming criteria are similar in nature to the polymer degradation phenomena and defect forming criteria occurring in the present paper.

A group of papers by Edirisinghe et al. address the similar case of diffusion of monomer through poly (α-methylstyrene) which decomposed to yield a high percentage of monomer. The decomposed monomer presented in the work of Calvert and Cima and that of Edirisinghe et. al. diffused through either pores or the liquid polymer. Models were developed which accounted for both types of diffusion [2-6]. The same criteria for bloating was employed in each case: bloating occurs when the monomer concentration is such that the pressure exceeds atmospheric pressure. A model similar in nature was developed for the present system and will be discussed in a separate paper [9,10].

Renlund and Johnson have patented an injection molding composition which utilizes SiC, EVA and stearic acid [11]. This is similar to the currently utilized system

which used EVA to spin filaments. The range of compositions which worked for Renlund et al. have been specified in the patent. They have stated that when the vinyl acetate part of the ethylene vinyl acetate copolymer is too low, surface cracks result. They attribute this to too high of a viscosity. However, it may be that the cause of the surface cracks are the result of the increased amount of crystallinity present in the material with less vinyl acetate content. There are large dimensional changes that take place upon crystallization and the higher the crystal content, the larger the dimensional changes as discussed by Hrdina [7, 12].

Renlund also noted that too much vinyl acetate content results in bloating during BBO. Although this was attributed to too low of a viscosity, it seems more likely that the cause of the bloating was the degradation of the EVA. The vinyl acetate initially degrades, as will be discussed shortly, to yield acetic acid. The more vinyl acetate, the more acetic acid formed at a given temperature. Therefore, it is likely that the bloating was simply a result of the increased amount of acetic acid formed as a result of the increased amount of vinyl acetate.

Ethylene Vinyl Acetate has the formula listed below. Upon heating in nitrogen, it first undergoes a side group elimination reaction [13-15], i.e.,

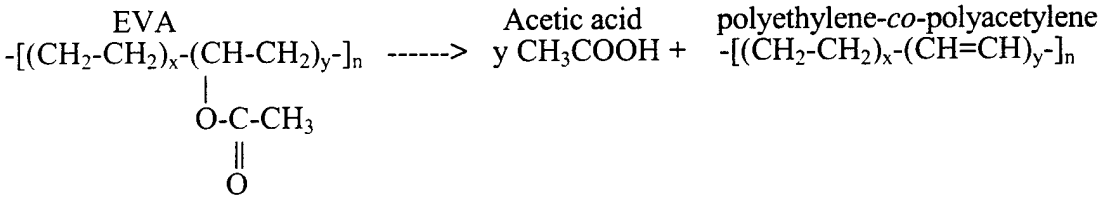

(Equation 1.)

This reaction is one of the primary reasons why this material was chosen for study. It yields a single well known and well characterized product in the first stage of the reaction. It needs to be emphasized that this well characterized reaction eliminates many uncertainties present in previously examined systems. The yield of acetic acid in the presence of the ceramic powder was shown to be almost 100% by gas chromatograph (GC) / mass spectrometry (MS) [8].

This reaction is well characterized and it has been suggested as a method to quantitatively analyzing the vinyl acetate content of EVA [14]. Fig. 1 compares the thermal gravimetric analysis (TGA) degradation behavior of polyethylene to that of EVA [13]. The vinyl acetate is eliminated at a much lower temperature than the temperature at which polyethylene begins to degrade. This results in what will be termed the "acetic acid shelf" in the TGA plot of EVA degradation. The remaining polymer will then be a copolymer of

polyethylene co-polyacetylene. Pure vinyl acetate will degrade to leave behind a conjugated polyacetylene structure [13] which is very stable.

Polyethylene, on the other hand, degrades by a random scission process. That is, because all bonds are essentially identical, there is no preferential degradation taking place, so that scission takes place randomly along the polymer chain [13,16,17].

2. Experimental procedures

2.1. Composition and processing

The single component moldable ceramic system examined here is composed of a pressureless sintering [18-21] composition of submicron SiC blended with a copolymer of ethylene and also, in some cases, mineral oil, a paraffinic distillate which is a common industrial. The powder is prepared by ball milling, using alumina grinding media, an isopropyl alcohol slurry composed of silicon carbide[1], aluminum oxide[2] and yttrium oxide[3] for 24 hours. The powder is next dried and ground to -40 mesh using a mortar and pestle.

Once the powder has been prepared it is then mixed in a heated blender[4] with the polymer or the polymer and mineral oil. The nominal room temperature volume percent ratios are 51/49 for the ceramic powder / co-polymer or 54.5 / 39.5 / 6 for ceramic powder / co-polymer / mineral oil respectively. Table I lists some of the properties of the pure polymer. The mixing head is first heated to 130°C, and the EVA copolymer[5] is added. After 1-2 minutes, the ceramic powder is added which then, because of the high shear, results in an increase in stock temperature to a final mixing temperatures of 150-160°C. The mineral oil[6], if used, is then added. The mixing speed is 60 RPM.

The binder uniformity in a batched material and between batches of material was checked by the random selection of four specimens from two separate batches of material. The percent of binder in each material was determined by TGA analysis. These results indicate no significant differences between binder content within a batch of material or between batches. The molding process may lead to preferential binder distribution if the polymer phase preferentially flows or is extruded away from high pressure regions leaving behind a powder rich phase [22,23]. The batched material was next molded at 27 MPa (4000 psi) in a uniaxial mold. TGA analysis on molded specimens revealed no difference

---

[1] B-SiC, H.C. Starck Grade B 10; SA = 14-17 m^2/g, mps = 0.75 um.
[2] Malakoff Industries, Inc., RC-HP DBM; SA=7-8 m^2/g, mps = 0.55 um.
[3] Johnson Matthey, mps = 1-2 um.
[4] C.W. Brabender Instruments, Inc., PL 2000 Plasti-Corder with Roller Blade Mixing Heads.
[5] ELVAX 470, Dupont.
[6] Heavy Mineral Oil, Mallinckrodt, Paraffin Oil, sp. = 0.881.

in the binder distribution throughout the specimen indicating that molding did not lead to any preferential binder distribution for this system.

2.2. Thermogravimetric measurements

Two different TGA units were employed. The first TGA[7] , utilized small 10-30 mg samples to study the degradation reaction kinetics of both the pure EVA and the EVA in the presence of the powder. The specimens were placed in a platinum pan and heated at constant heating rate to determine the reaction kinetics. The second TGA[8] utilized larger specimens in which mass transport was considered to be rate limiting.

2.3. Hot-stage microscopy (bubble formation in pure EVA)

Bubble formation in EVA was observed by hot-stage microscopy, similar to previous work by Dong and Bowen [24] in which they examined bubble formation in PMMA mixed with different solvents. Pure EVA 470 was placed between two metal sheets, heated to 125°C and then molded into a 0.5 mm thick sheet, and cut into 4 mm disks. The EVA disks were sandwiched between two glass disks 6 mm in diameter. The glass disks were cut from 1 mm glass slides and washed with isopropyl alcohol before use. The sandwiched assembly was placed within a controlled atmosphere hot-stage microscope[1] and observed with transmitted light. The specimen was then heated at 2°C/min in a nitrogen atmosphere to about 350°C while recording the image with a video camera. In a second experiment, EVA was seeded by mixing approximately 0.05 weight percent of 90 weight percent SiC, 6 weight percent aluminum oxide and 4 weight percent yttrium oxide powder. This small amount of powder was not enough to make the system opaque. However, it still provided many particles or possible sites for bubble formation . The particle density was approximated at 2×10^{12} particles / cm^3 based on equivalent spherical diameters. This material was molded into sheets, cut, sandwiched and placed in the microscope in the same manner as the unseeded pure EVA 470 polymer.

It was discovered that in all cases, a bubble which formed grew rapidly and could be seen with the unaided eye within a few seconds of forming. This was recorded as the bubble formation temperature.

2.4. Bloating maps

---

[7] TA Instruments Hi-Res TGA 2950.
[8] TGA-171, ATI-CAHN microbalance.
[1] Linkam TH1500.

A number of experiments were run to determine the effect of heating rate and sample size on bloating in the molded specimens. The objective of these experiments was to provide a data base of bloating conditions. The experimental conditions under which bloating takes place is presented here.

Ceramic powder / EVA was compressed in a uniaxial mounting press at 125°C and 27 MPa. Specimens were 25.4 mm in diameter and varied in thickness between 0.5 mm and 8 mm. The specimens were in the mold for 15 minutes at 125°C temperature to anneal out most of the residual strains reported in another paper [7].

Fig. 2 shows an example of the specimen set-up. The specimens are shown on a setter plate before heating. The upright placement allowed diffusion through both faces of the specimen which approximated planar diffusion. The specimens were then heated at constant heating rates to a specified temperature and furnace cooled to room temperature. Most bloating was readily apparent from the surface. However, all specimens were cut into several pieces to visually inspect for internal cracking or bloating. The minimum bloating temperature was determined to within 20°C.

3. Results and discussion

3.1. Bubble formation in pure polymer

Bubbles were observed to form in the specimens at temperatures between 286°C and 310°C as shown in Table 8.1. The first bubble that formed grew quickly and appeared typically in proximity to the center region of the disk. As the specimen was heated further, a second or third bubble might form, but always at a relatively large distance (~0.5 mm or more) away from the first bubble. Shown in Fig. 3 is an optical image of a seeded specimen before and after a bubble was observed to form. Seeding did not appear to change the nature of bubble formation. The bubbles formed and grew in the same manner as the pure EVA polymer.

Pure acetic acid is a product of the elimination reaction of EVA and is forming during heating throughout the polymer as a dissolve gas (acetic acid boils at 118°C). A TGA trace of pure EVA at 2°C/min can be seen in Fig. 4. At 286°C, only 1.3 weight % of the total organic has decomposed and at 310°C, 4.5% has decomposed. It is apparent that bubble formation is associated with the beginning of polymer degradation. In a covered slide, generated acetic acid has one escape route, through the polymer to the specimen edge, where it then evaporates. However, if it forms faster then it can escape, a

concentration of acetic acid will build up. If the concentration exceeds a critical value, a bubble can form.

It appears that the bubble formation requires a favorable formation site. If this were not true, then bubble formation would always start in the exact center of the specimen, at the point of highest concentration of acetic acid. The distribution in the temperature at which bubbles form also suggests that favorable bubble formation sites are not readily available in the pure polymer. Additionally, the ceramic powder does not appear to act as a favorable site for bubble formation because the bubbles still appear to form over a range of temperatures and in a generally central region.

Once a bubble forms, it then appears to act as a sink for diffusing acetic acid species. Others reported similar behavior [25-28]. A schematic of this behavior is presented in Fig. 5. The only sink for the diffusing species is, initially, the surface. It is speculated that acetic acid concentration must build up in the specimen's central region past the point of saturation because favorable bubble formation sites are not available [27]. Once a bubble does form, it then acts as a sink for acetic acid in the surrounding material [26,27]. Other bubble formation must then take place at distances relatively far away from the two sinks which are the surface and the already present bubbles.

These results indicate that bubbles form within pure EVA and are the result of internal pressure from acetic acid. Acetic acid is the product of the thermal degradation reaction of EVA. The results also indicate that some amount of acetic acid supersaturation is required because of a lack of favorable sites for bubble formation. Therefore, a necessary condition for bubble formation is:

(1) $a_{\text{acetic acid}} P_o > P_{\text{atmosphere}}$

where: $a_{\text{acetic acid}}$ is the activity of acetic acid in the polymer
P_o is the equilibrium vapor pressure of acetic acid over a free surface and
$P_{\text{atmosphere}}$ is atmospheric pressure.

No bloating will occur unless this minimum or necessary condition is first met.

3.2. Bubble formation in filled system

The bubble formation in pure EVA appeared to be the result of acetic acid exceeding a critical concentration. This is the primary cause of defects in this moldable system. The primary objective of this section is to confirm that the observed bloating is a result of acetic

acid which has exceeded a critical concentration. Two secondary objectives are also examined. First, the effect of mineral oil on bloating in this system is discussed. It is speculated that mineral oil does not contribute to bloating. Finally, it was observed that bloating was effected by molding pressure. A possible explanation for these results will be discussed.

3.2.1. *Conditions for bloating*

The defects that show up appear to start as an internal crack, and then develop into bloats as a result of the acetic acid exceeding a critical concentration. A typical example of a defect observed in the present system is shown in Fig. 6. This particular specimen is 3 mm thick and was heated at 2°C/min to 270°C and cooled. Two rather large bubbles are shown that appear near the center of the specimen. Duplicate specimens heated to 250°C at the same rate did not bloat.

It should be remembered that acetic acid is forming everywhere in the material during heating. It was also shown in a previous paper that acetic acid does diffuse through the system to the surface[8]. Therefore, the region of highest concentration is expected to be the specimen center which has the longest diffusion path. This is also the primary region where bloating is observed. The bloating is also associated with the initial region of weight loss. Acetic acid was found to be the overwhelming product of the reaction in this region as was reported previously in a paper describing the chemistry of degradation in this system [8].

Most bubbles within the filled specimens occur near the center of the specimen, but location varies somewhat from specimen to specimen and from bubble to bubble within a center. This suggests that a minimum supersaturation appears required for formation of a bubble. Large bubbles also suggest that once a bubble forms, it then acts as a sink for diffusing species like in the case of the pure polymer.

Fig.'s 7a and 7b are scanning electron micrographs (SEM) of a bloating defect formed in a 2 mm thick specimen that was heated at 2°C/min to 320°C and had 4.3% of its binder removed. The crack was not visible from the specimen surface. The specimen had to be cut open to view the crack and like the previous specimen, the crack again appeared in the specimen center. No cracks were observed throughout the rest of the cross section or in the surrounding region.

Similar behavior is found in the filled EVA system as in the filled EVA system with mineral oil. It appears that additions of up to 6% mineral oil (BP =346°C) does not affect the acetic acid induced bloating behavior.

3.2.2. *Demonstration that acetic acid can cause bloating*

An experiment was performed in which external acetic acid was added to the specimen, which caused bloating during subsequent heating. A molded 2 mm specimen was soaked in pure liquid acetic acid at room temperature for 9 days. The amount of acetic acid absorbed in the filled specimen was equivalent to about 21 percent of the polymer's weight. The specimen was heated at 2°C/min to 150°C, well below the temperature at which acetic acid forms by the elimination reaction, but well above the boiling point of acetic acid of 118°C. The results are shown in Fig. 8 for the specimen before and after heating. It is evident that the specimen bloated. Note also that bloating occurs almost precisely in the specimen center.

3.2.3. *Effect of molding pressure on bloating*

Pieces of 2 mm rods of the SiC/EVA compound were compression molded into rectangular billets. 51 volume percent ceramic and 49 volume percent EVA was extruded[9] into 2 mm diameter rods. The extrudate was cut into 25 mm lengths and about 20 pieces were placed in a die. Three billets 50 mm x 25 mm x 9 mm were fabricated by pressing at 150°C at pressures of 1.7 MPa, 3.5 MPa and 35 MPa respectively. The specimens were then placed side by side in a furnace and heated in a nitrogen atmosphere according to the following schedule: 1°C/min to 145°C. Then 0.03°C/min to 250°C and 0.07°C/min to 300°C. Each specimen lost 10% of its organic content. Fig. 9 shows the results of the experiment. The specimen compression molded at 1.7 MPa bloated badly. The specimen molded at 3.5 MPa shows much less bloating. The specimen pressed at 35 MPa did not appear to bloat at all. The only difference between the initial specimen was the molding pressure. It is clear that bloating defects were minimized and or avoided by employing higher molding pressures.

Bloating originates at the weld lines in these samples. The bloated region observed in the specimen pressed at 3.5 MPa in Fig. 9 seems to partially trace the exterior of a 2 mm diameter extruded specimen. This bloat, therefore seems to suggest that bloating is occurring at a weld line. Additionally, breaks in the weld line at the surface of the specimen pressed at 1.7 MPa are clearly seen in Fig. 9 which indicate that the weld lines are regions where fracture occurs.

---

[9] Bradford University Ltd. extruder.

The strength of weld lines in injection molded parts increases with increasing molding pressure [30]. This is assumed to be the case here as well. It seems plausible, that once the condition of supersaturation was achieved, the weak weld lines in the 1.7 MPa pressed specimen yielded before the weld lines in the other specimens and acted as a sink for further diffusing acetic acid species.

3.3. Bloating maps

"Bloating maps" displaying the temperature at which bloating occurs vs. specimen size and heating rate were prepared. Fig. 10a plots the minimum temperature at which bloating was observed for various size specimens heated at 8°C/min. Bloating occurs in the region above the curve does not occur in the region below the curve. Fig. 10b summarizes three different heating rates on the same plot. The data in Fig. 10b is plotted for constant heating rates of 0.5°C/min, 2°C/min and 8°C/min. It is apparent that thicker specimens bloat at lower temperatures. It is also apparent that bloating temperature decreases with increasing heating rate.

These data can be combined with the acetic acid generation rate, obtained from TGA traces on small 25 mg samples at the specified temperature and heating rate, with the data of Fig. 10. This is displayed in Fig. 11 as acetic acid generation rate versus sample thickness. It is apparent that the data for all three heating rates appears to collapse into a single curve so that the single line that differentiates the bloating region from the no bloat region could be termed the critical generation rate, $G_{critical}$. Diffusion is approximated by the generation rate and the diffusion distance, x, is half the specimen thickness. Fig. 11 shows the generation rate versus diffusion distance squared. The results of Fig. 11 suggests the presence of two regimes.

The explanation of the regimes is better illustrated with use of schematic concentration profiles shown in Fig. 12. Within Regime #1, the specimens appear to all bloat at roughly the same low critical generation rate. Diffusion in these large samples is so low that almost all generated species accumulate in the specimen center in this regime. Bloating then occurs as soon as enough acetic acid is accumulated such that the critical concentration is exceeded. Within Regime #2, the diffusion distance in the thin specimens is small enough so that all that is generated is not accumulated. Bloating in this regime is controlled by a competition between diffusing species leaving the system and generated species added to the system. The rate of generation of acetic acid must exceed the rate at which it diffuses and the distance through which it has to diffuse in order to have accumulation. Bloating occurs when the amount accumulated exceeds the critical

concentration. These maps form the data base that will be used in a model presented elsewhere [9,10].

3.4. Conclusions

Bubble formation during heating was observed in pure EVA. The evidence strongly suggests that bubble formation is from acetic acid exceeding a critical level. The minimum condition for bloating is when the internal pressure exceeds atmospheric pressure such that:
$a_{\text{acetic acid}} P_o > P_{\text{atmosphere}}$. A second but less defined criteria for bloating involved finding a favorable site for bubble formation. Seeding the system with ceramic powder did not appear to change the mechanism for bubble formation. Nor did the powder appear to appreciably alter the likelihood of bubble formation at a specific temperature.

Bloating in filled systems also appears to be the result of acetic acid concentration exceeding a critical value. It was proven that external addition of acetic acid did cause bloating in the filled system in the same manner as in the filled systems which form acetic acid. Experimental results showed that bloating defects could be minimized or avoided in some cases by employing higher molding pressures. The mechanism by which molding pressure affected defect formation is the subject of future work.

Bloating maps were presented and provide criteria under which defects could be avoided in the present system. The results seem to collapse into a single curve such that a critical rate of generation of acetic acid, G_{critical} is obtained for any specific sample thickness. Bloating occurs if G_{critical} is exceeded. It appears that two bloating regimes exist. The first regime is for large size samples where diffusion is so low that all acetic acid that is generated is accumulated. This is the diffusion controlled regime. The second regime occurs for smaller size specimens where diffusion is fast enough such that generated species are leaving the central region of the specimen at an appreciable rate. Accumulation of species occurs only when the rate of generated species exceeds the rate at which they diffuse away from the specimen. Bloating in this region is controlled by the competition between rate of generation of acetic acid and diffusivity of acetic acid.

ACKNOWLEDGMENT

This research was supported by the Defense Advanced Research Projects Agency and the Office of Naval Research through grant N00014-94-1-0278.

TABLE I Selective properties of EVA 470

Melt index: 0.7 dg/min	M_n = 100,000 M_w = 250,000	T_g = -20°C T_m = 84°C
Density = 0.941 g/cm^3	FORMULA $-[(CH_2-CH_2)_x-(CH-CH_2)_y-]_n$ $\lvert$ $O-C-CH_3$ $\lVert$ O	Percent Crystalline = 10% vinyl acetate (VA) content = 18wt%

Table II Observed temperatures of bubble formation

Specimen	Observed Temperatures of Bubble Formation
Pure EVA	**303°C ± 3°C**
Seeded EVA	**298°C ± 12°C**

4. References

1. P. Calvert and M. Cima, J. Amer. Ceram. Soc., **73** [3] (1990) 575.
2. J.R.G. Evans, M.J. Edirisinghe, J.K. Wright, and J. Crank, Proc. Royal Society London, A **432** (1991) 321.
3. H.M. Shaw and M.J. Edirisinghe, Philosophical Magazine, A, **72** [1] (1995) 267.
4. S.A. Matar, J.R.G. Evans, M.J. Edirisinghe, and E.H. Twizell, J. Mater. Res., **10** [8] (1995) 2060.
5. E.H. Twizell, S.A. Matar, D.A. Voss, and A.Q.M. Khaliq, Int. J. Eng. Sci., **30** [3] (1992) 379.
6. S.A. Matar, M.J. Edirisinghe, J. R.G. Evans, and E.H. Twizell, J. Amer. Ceram. Soc., **79** [3] (1996) 749.
7. K.E. Hrdina and J.W. Halloran, J. Mater. Sci., submitted 1997.
8. K. E. Hrdina, J.W. Halloran, M. Kaviany, and A. Oliveira, J. Mater. Sci., submitted 1997.
9. A.M. Oliveira, K.E. Hrdina, M. Kaviany, and J.W. Halloran, J. Mater. Sci., submitted 1997.
10. A.M. Oliveira, K.E. Hrdina, M. Kaviany, and J.W. Halloran, 1997 National Heat Transfer Conference, Baltimore, MD, August 10-12, 1997, submitted.
11. G. Renlund and C. Johnson, US PATENT # 4,571,414 (1986).
12. K.E. Hrdina, in "Phenomena During Thermal Removal of Binders" (Ph.D. Thesis, University of Michigan, May, 1997).
13. H.H.G. Jellinek, in "Degradation of Vinyl Polymers" (Academic Press, Inc., NY 1955) chapter 2.
14. R.J. Koopmans, R. Van Der Linden, and E.F. Vansant, Poly. Eng. and Sci., **22** [14] (1982) 878.
15. I.M.Salin and J.C.Seferis, J. Appl. Poly. Sci., **47** (1993) 847.
16. E.M. Pearce, C.E. Wright and B.K. Bordoloi, in "Laboratory Experiments in Polymer Synthesis and Characterization" (Penn State University, 1982).
17. S.L. Madorsky, in "Thermal Degradation of Organic Polymers" (Interscience Publishers, NY, 1964) chapters IV and VI.
18. M.A. Mulla and V.D. Krstic, Ceram. Bul., **70** [3], (1991) 439.
19. M.A. Mulla and V.D. Krstic, J. Mater. Sci., **29**, (1994) 934.
20. Do-Hyeong Kim and Chong Hee Kim, J. Amer. Ceram. Soc., **73** [5] (1990) 1431.
21. V.D. Krstic personnel contact October, 1994.
22. R. German, in " Powder Injection Molding" (Metal Powder Industry Federation, Princeton, 1990) chapter 10.
23. B.O. Rhee, M.Y. Cao, H.R. Zhang, E. Streicher, and C.I. Chung, Powd. Inject. Mold. (1991) 43.
24. C. Dong and H.K. Bowen, J. Amer. Ceram. Soc., **72** [6] (1989) 1082.
25. J.R. Wood and M.G. Bader, J. Mater. Sci., **30** (1995) 916.
26. J.R. Street, A.L. Fricke, and L.P. Reiss, Ind. Eng. Chem. Fundam., **10** [1] (1971) 54.
27. M.S. Plesset and S.A. Zwick, J. Appl. Phys., **25** [4] (1954) 493.
28. I. Wichman, Combust. and Flame, **63** (1986) 217.
29. Mineral Oil Product Bulletin Form 30.221 (2).
30. I. Rubin, in "Injection Molding, Theory and Practice" (John Wiley & Sons, New York, 1972) p. 440.

List of Figures

Fig. 1 TGA of pure EVA compared to pure polyethylene.

Fig. 2 Specimen set-up for mapping bloating conditions.

Fig. 3 Observed bubble formation in hot-stage optical microscope of seeded EVA sample sandwiched between two glass slides.

Fig. 4 TGA of pure EVA at constant heating rates.

Fig. 5 Schematic of diffusing zones during thermal degradation of EVA within hot-stage microscope.

Fig. 6a Defect observed in current system.
6b TGA trace showing defect occurs during initial weight loss.

Fig. 7 SEM of bloated region.
7a low magnification.
7b higher magnification of crack tip.

Fig. 8 Bloating as a result of external addition of acetic acid.

Fig. 9 Effect of molding pressure on bloating.

Fig. 10 Bloating maps.
10a Effect of sample size with single heating rate of 8°C/min.
10b Effect of sample size and heating rate with heating rates of 0.5°C/min, 2°C/min and 8°C/min.

Fig. 11 Bloating maps at various heating rates collapse into a single bloating map with two bloating regimes shown.

Fig. 12 Schematic representation of acetic acid concentration profiles in two bloating regimes.

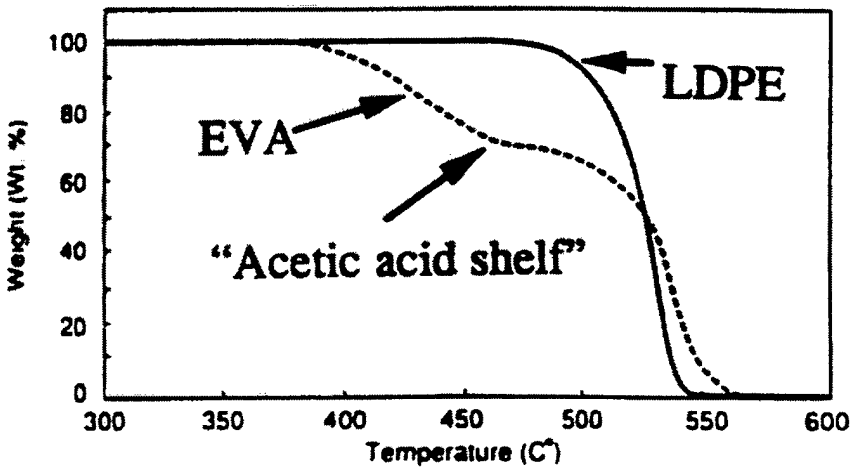

Fig. 1

Hrdina, Halloran, Kaviany & Oliveira

Cylindrical specimens 25.4 mm diam.: thickness, t

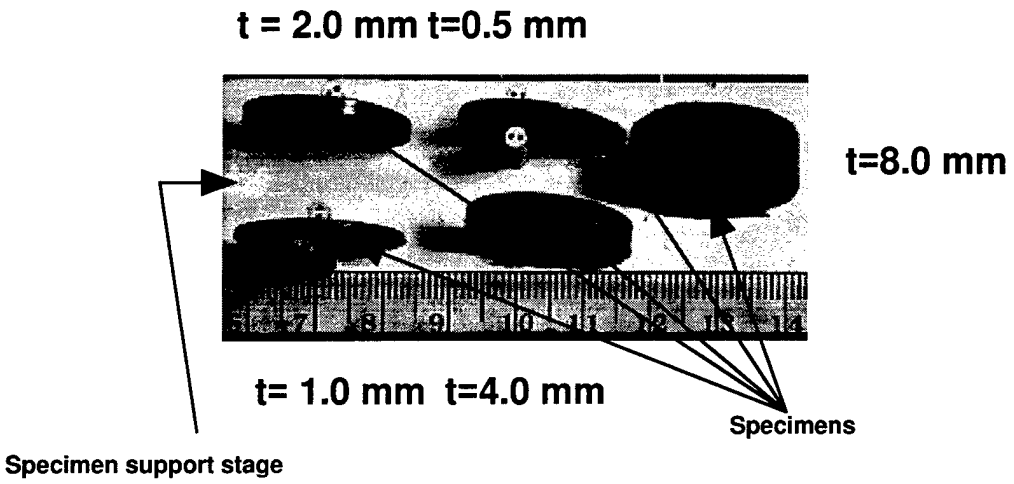

Fig. 2

Hrdina, Halloran, Kaviany & Oliveira

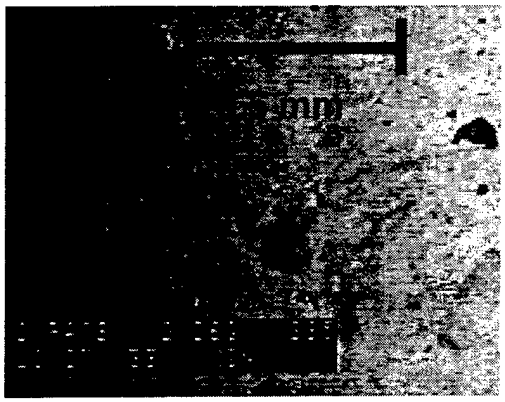

T=285 °C

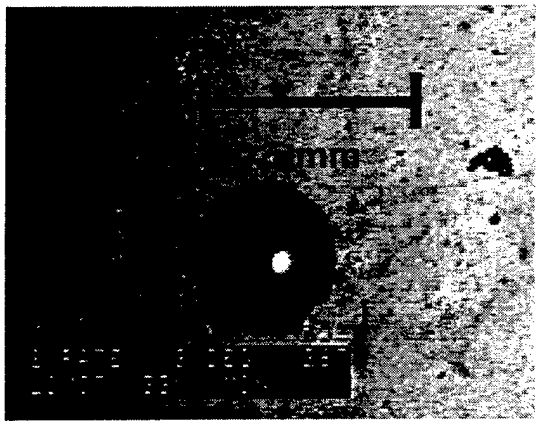

T= 287 °C
1 minute later.

Fig. 3

Hrdina, Halloran, Kaviany & Oliveira

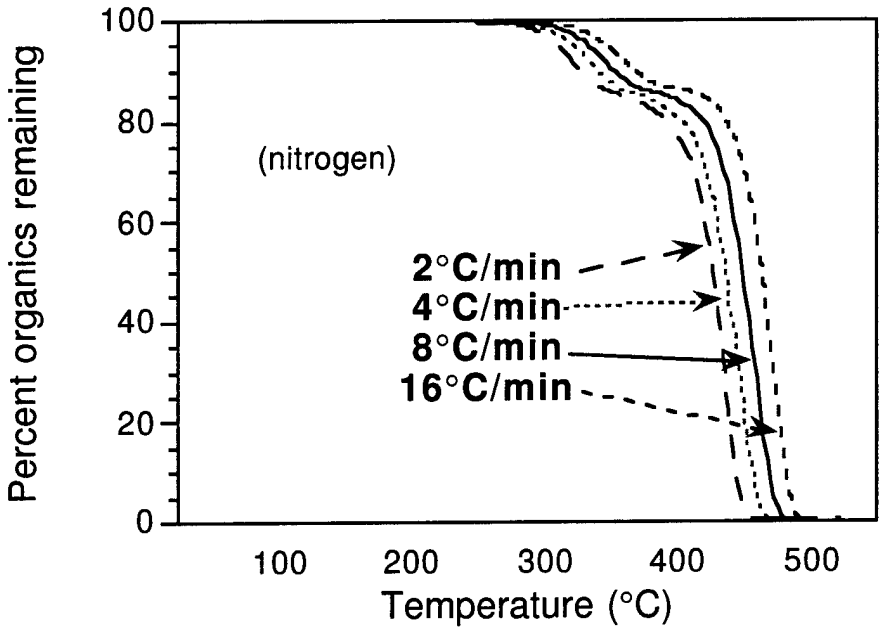

Fig. 4

Hrdina, Halloran, Kaviany & Oliveira

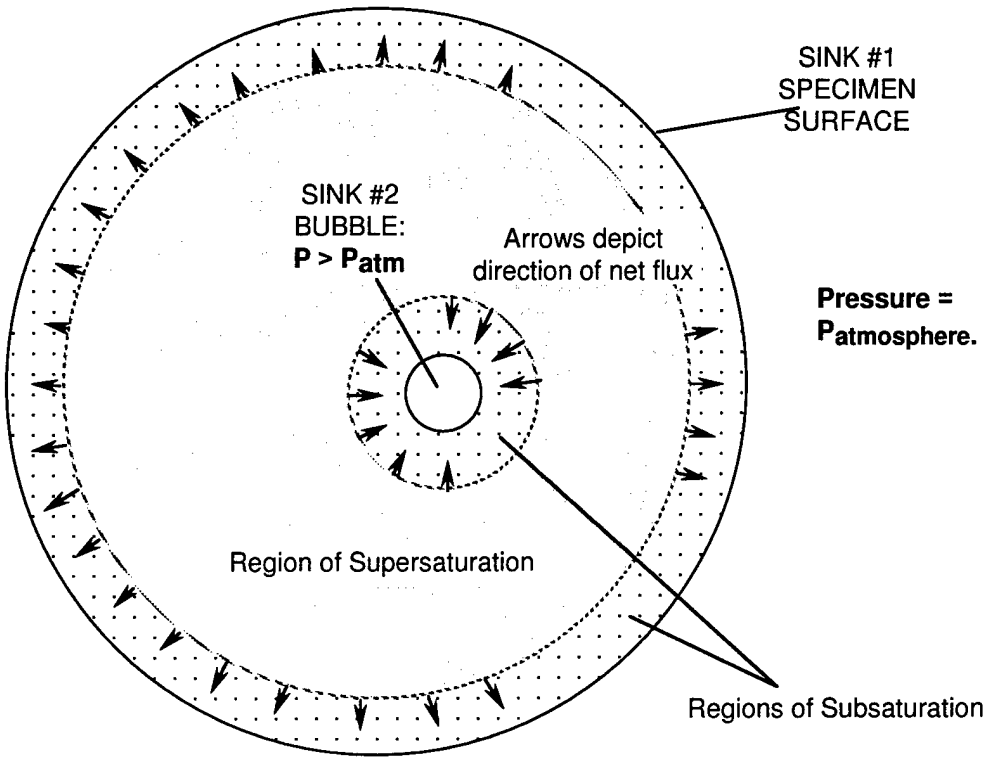

Fig. 5

Hrdina, Halloran, Kaviany & Oliveira

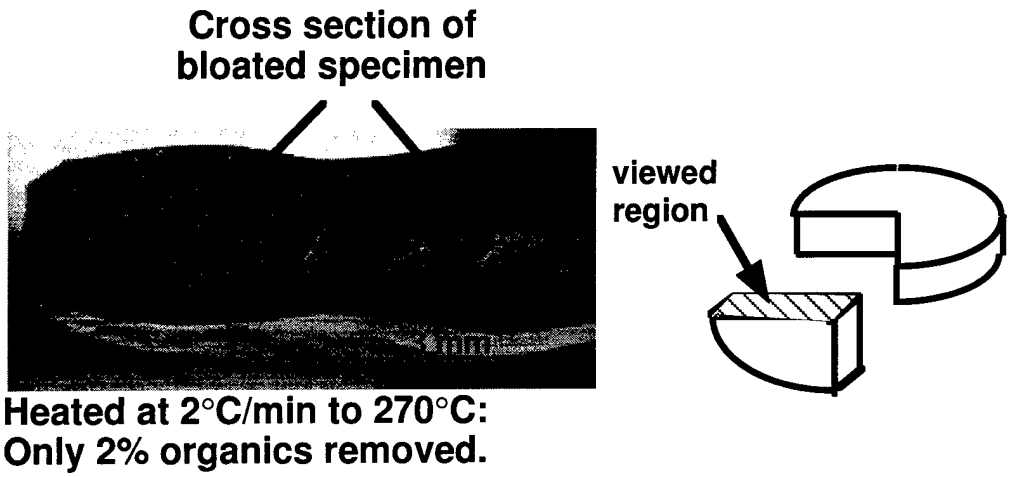

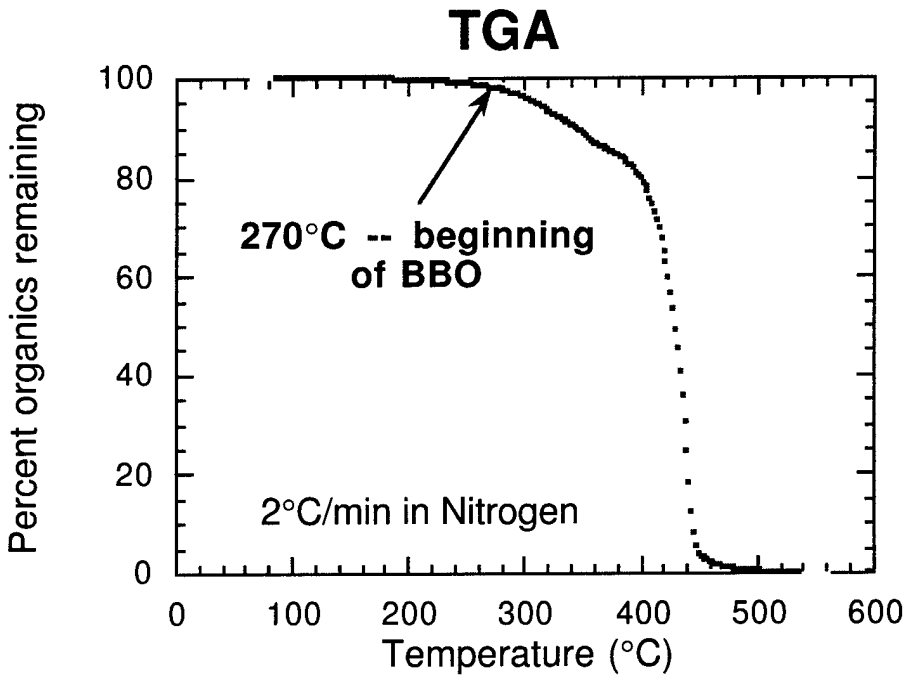

Fig. 6a & b

Hrdina, Halloran, Kaviany & Oliveira

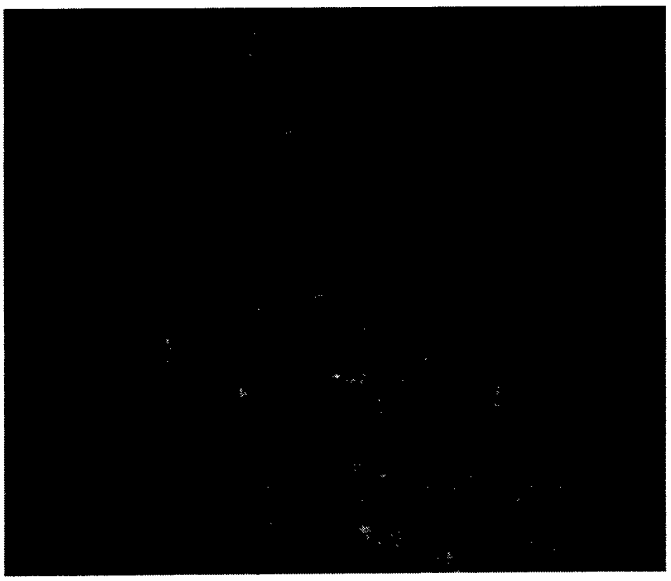

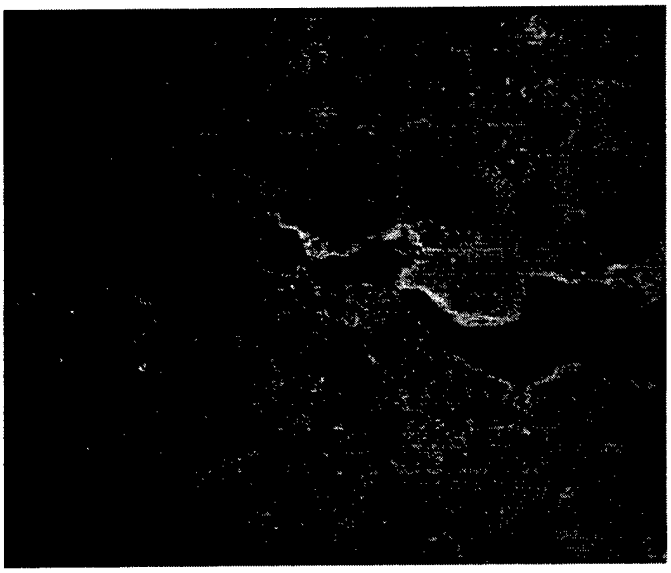

Fig. 7a & b

Hrdina, Halloran, Kaviany & Oliveira

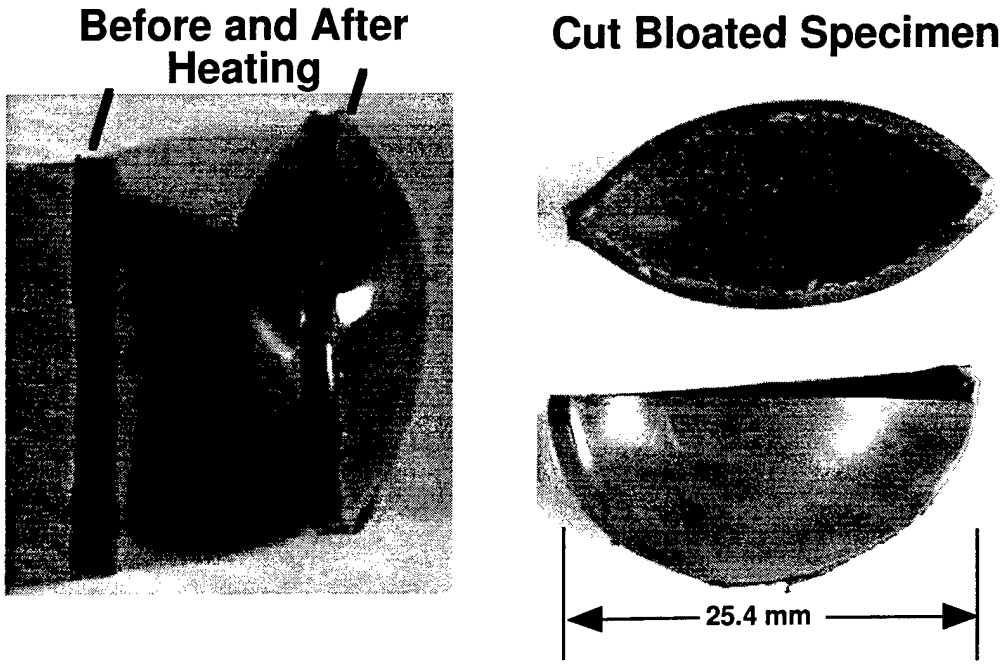

Fig. 8
Hrdina, Halloran, Kaviany & Oliveira

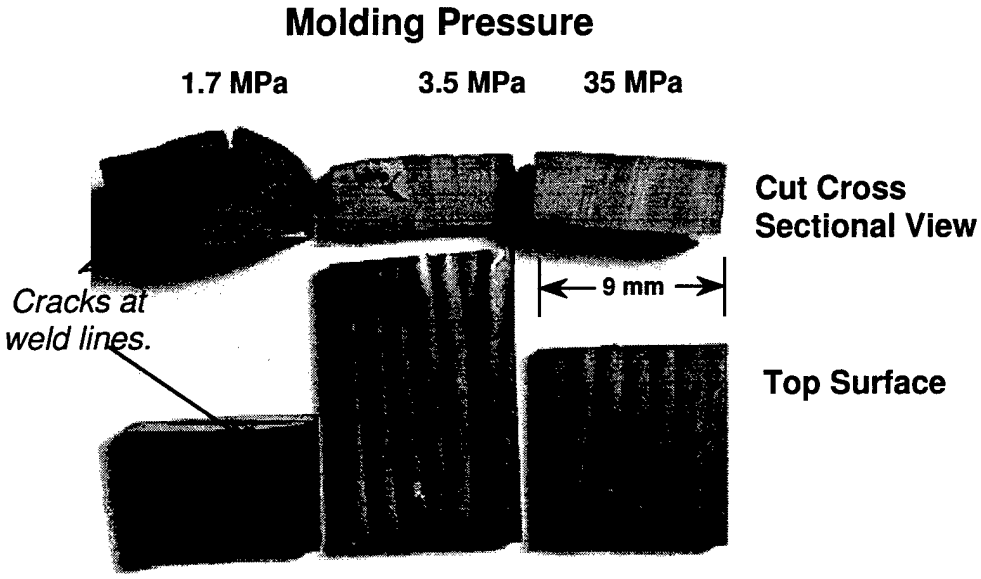

Fig. 9
Hrdina, Halloran, Kaviany & Oliveira

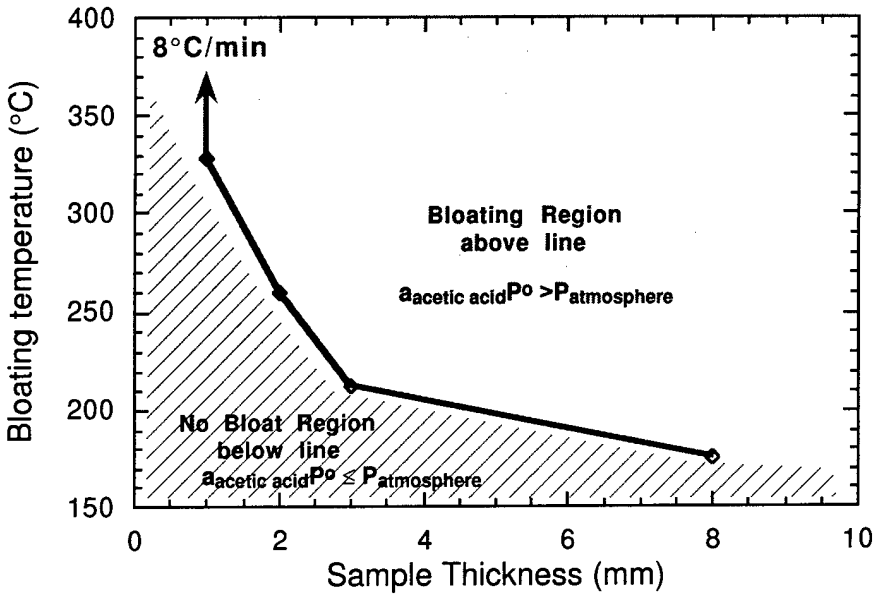

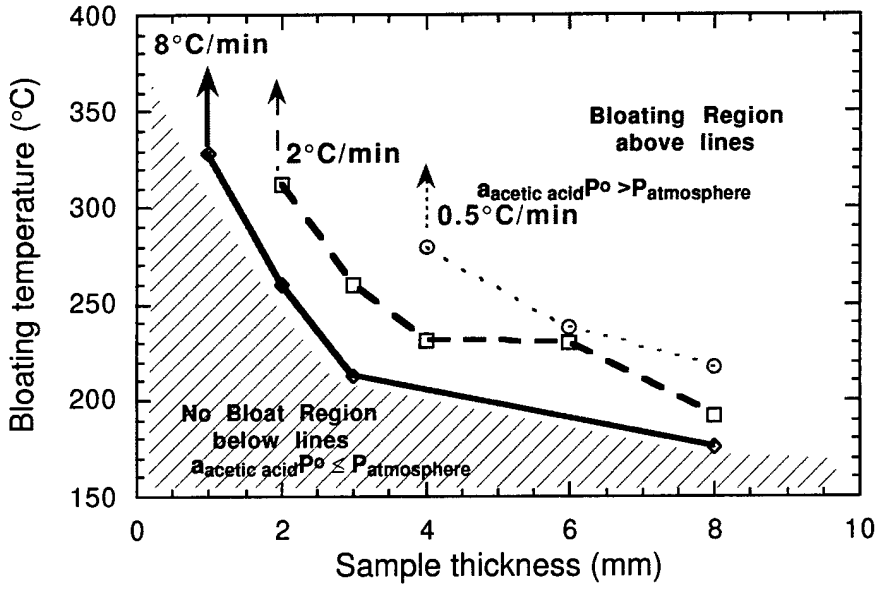

Fig. 10a & b

Hrdina, Halloran, Kaviany & Oliveira

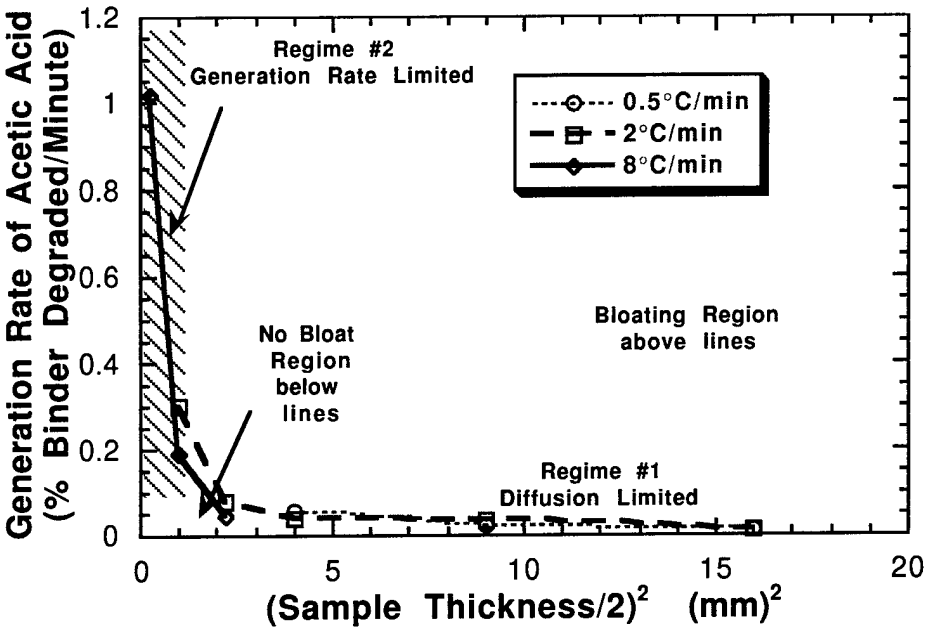

Fig. 11

Hrdina, Halloran, Kaviany & Oliveira

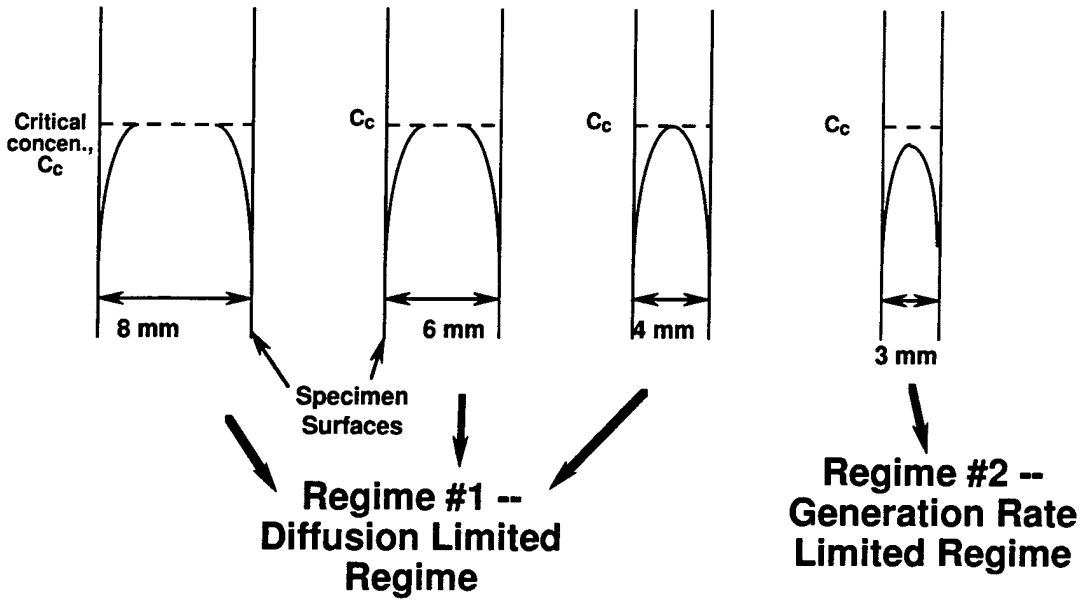

Fig. 12
Hrdina, Halloran, Kaviany & Oliveira

REPORT DOCUMENTATION PAGE

Form Approved
OMB No. 0704-0188

1. AGENCY USE ONLY (Leave blank)	2. REPORT DATE	3. REPORT TYPE AND DATES COVERED
	August 25, 1997	Final Report 4/1/94 - 3/30/97

4. TITLE AND SUBTITLE

Net Shape Forming of Tough Fibrous Monolithic Ceramics

5. FUNDING NUMBERS

N00014-94-1-0278

6. AUTHOR(S)

John W. Halloran

7. PERFORMING ORGANIZATION NAME(S) AND ADDRESS(ES)

University of Michigan
Division of Research Development Administration
1058 Wolverine Tower
3003 South State St.
Ann Arbor, MI 48109-1274

8. PERFORMING ORGANIZATION REPORT NUMBER

9. SPONSORING/MONITORING AGENCY NAME(S) AND ADDRESS(ES)

Steven G. Fishman
Office of Naval Research
800 North Quincy St.
Arlington, VA 22217-5660

10. SPONSORING/MONITORING AGENCY REPORT NUMBER

11. SUPPLEMENTARY NOTES

12a. DISTRIBUTION/AVAILABILITY STATEMENT

Unlimited public availability

12b. DISTRIBUTION CODE

13. ABSTRACT *(Maximum 200 words)*

Significant dimensional changes involving linear expansion and shrinkage of 6% occur during heating of a thermoplastic SiC/ethylene vinyl acetate mixture. Thermal expansion occurs before weight loss begins, and can be quantitatively explained in terms of the thermal expansion behavior of the constituents and the crystallization or melting of the semicrystalline polymer. Irreversible anisotropic displacements occur during the first heating cycle due to relaxation of molding strains. These can be reduced by annealing for periods comparable to the viscoelastic relaxation of the ceramic/polymer system. Shrinkage occurs during the early stages of degradation of EVA. This shrinkage is quantitatively accounted for with volume losses resulting from removal of the EVA. Shrinkage continues as weight loss proceeds and stops only at the point the ceramic particles contact one another. Total displacement behavior is the sum of the shrinkage from weight loss plus the expansion from thermal expansion of the individual components, and can be quantitatively predicted for simple or multi-step heating schedules.

14. SUBJECT TERMS

binder, removal, dimension, ceramic composites, fabrication, polymer pyrolysis, binder burnout

15. NUMBER OF PAGES

101

16. PRICE CODE

17. SECURITY CLASSIFICATION OF REPORT	18. SECURITY CLASSIFICATION OF THIS PAGE	19. SECURITY CLASSIFICATION OF ABSTRACT	20. LIMITATION OF ABSTRACT
unclassified	unclassified	unclassified	unlimited

GENERAL INSTRUCTIONS FOR COMPLETING SF 298

The Report Documentation Page (RDP) is used in announcing and cataloging reports. It is important that this information be consistent with the rest of the report, particularly the cover and title page. Instructions for filling in each block of the form follow. It is important to ***stay within the lines*** to meet ***optical scanning requirements.***

Block 1. Agency Use Only *(Leave blank)*.

Block 2. Report Date. Full publication date including day, month, and year, if available (e.g. 1 Jan 88). Must cite at least the year.

Block 3. Type of Report and Dates Covered. State whether report is interim, final, etc. If applicable, enter inclusive report dates (e.g. 10 Jun 87 - 30 Jun 88).

Block 4. Title and Subtitle. A title is taken from the part of the report that provides the most meaningful and complete information. When a report is prepared in more than one volume, repeat the primary title, add volume number, and include subtitle for the specific volume. On classified documents enter the title classification in parentheses.

Block 5. Funding Numbers. To include contract and grant numbers; may include program element number(s), project number(s), task number(s), and work unit number(s). Use the following labels:

C	- Contract	**PR**	- Project
G	- Grant	**TA**	- Task
PE	- Program Element	**WU**	- Work Unit Accession No.

Block 6. Author(s). Name(s) of person(s) responsible for writing the report, performing the research, or credited with the content of the report. If editor or compiler, this should follow the name(s).

Block 7. Performing Organization Name(s) and Address(es). Self-explanatory.

Block 8. Performing Organization Report Number. Enter the unique alphanumeric report number(s) assigned by the organization performing the report.

Block 9. Sponsoring/Monitoring Agency Name(s) and Address(es). Self-explanatory.

Block 10. Sponsoring/Monitoring Agency Report Number. *(If known)*

Block 11. Supplementary Notes. Enter information not included elsewhere such as: Prepared in cooperation with...; Trans. of...; To be published in.... When a report is revised, include a statement whether the new report supersedes or supplements the older report.

Block 12a. Distribution/Availability Statement. Denotes public availability or limitations. Cite any availability to the public. Enter additional limitations or special markings in all capitals (e.g. NOFORN, REL, ITAR).

- **DOD** - See DoDD 5230.24, "Distribution Statements on Technical Documents."
- **DOE** - See authorities.
- **NASA** - See Handbook NHB 2200.2.
- **NTIS** - Leave blank.

Block 12b. Distribution Code.

- **DOD** - Leave blank.
- **DOE** - Enter DOE distribution categories from the Standard Distribution for Unclassified Scientific and Technical Reports.
- **NASA** - Leave blank.
- **NTIS** - Leave blank.

Block 13. Abstract. Include a brief *(Maximum 200 words)* factual summary of the most significant information contained in the report.

Block 14. Subject Terms. Keywords or phrases identifying major subjects in the report.

Block 15. Number of Pages. Enter the total number of pages.

Block 16. Price Code. Enter appropriate price code *(NTIS only)*.

Blocks 17. - 19. Security Classifications. Self-explanatory. Enter U.S. Security Classification in accordance with U.S. Security Regulations (i.e., UNCLASSIFIED). If form contains classified information, stamp classification on the top and bottom of the page.

Block 20. Limitation of Abstract. This block must be completed to assign a limitation to the abstract. Enter either UL (unlimited) or SAR (same as report). An entry in this block is necessary if the abstract is to be limited. If blank, the abstract is assumed to be unlimited.